

Online Appendix for "Industry Input in Policymaking:
Evidence from Medicare"

David C. Chan and Michael J. Dickstein

January 29, 2019

I	Setting the Medicare Budget	1
II	Measuring Affiliation	2
	Euclidean Distance Metrics	2
	Alternative Distance Metrics	5
	Cross-Service Spillovers	6
III	Mixed Strategies in Endogenous Proposals	7
IV	Quasi-Experimental Variation in Affiliation	9
	Quasi-Experimental Variation in \mathcal{R}_t	9
	Quasi-Experimental Variation in \mathcal{S}_i	10
V	Counterfactual Revenue Analysis	12
	Simulation Algorithm	12
	Distribution of Counterfactual Affiliations	13
VI	Alternative Mechanisms Behind the Price Effect	13
VII	Heterogeneous Effect of Affiliation by Proposal Type	15
VIII	Technical Details of the Conceptual Framework	15
	Canonical Crawford and Sobel (1982) Partitions	16
	Hard Information	17
	Optimal RUC Bias	18
	Uniform Posterior Intervals	19
IX	Private Price Transmission Robustness	20

I Setting the Medicare Budget

This appendix summarizes the process that sets the overall Medicare budget for physician services, which equivalently determines the conversion factor, or CF_t in Equation (1). We focus on the period between the Balanced Budget Act of 1997 and the Medicare Access and CHIP Reauthorization Act of 2015. A more extensive discussion of this process can be found elsewhere (e.g., American Medical Association, 2015; Centers for Medicare and Medicaid Services, 2014). During this period, CMS set CF_t according to the following formula:

$$CF_t = CF_{t-1} \times (1 + MEI_t) \times (1 + UAF_t) \times BN_t,$$

where MEI_t is the Medicare Economic Index, UAF_t is the Update Adjustment Factor, and BN_t is the Budget Neutrality adjustment.

MEI_t is the weighted-average price change for inputs required to operate a self-employed physician practice in the United States. The measure indexes inflation for medical services. There are two broad categories of inputs: the physician's own time and his or her practice expense. The MEI Technical Advisory Panel continually reviews and updates the index, recommending changes to ensure that MEI_t appropriately meets its statutory purpose.

UAF_t is a mechanism that keeps Medicare spending at an acceptable level given real gross domestic product per capita and year-to-year changes in fees and beneficiaries. The current year's target expenditures are equal to target expenditures in the previous year adjusted by the Sustainable Growth Rate (SGR_t). The update also compares actual expenditures with target expenditures from April 1, 1996 through the preceding year. By federal statute, $UAF_t \in [-7\%, 3\%]$, and the formula for the UAF_t is based on the following identities, relating target and actual spending:

$$\begin{aligned} \sum_{t'=1}^t \text{Target}_{t'} &= \sum_{t'=1}^t \text{Actual}_{t'}; \\ \text{Actual}_t &= \text{Actual}_{t-1} \times (1 + SGR_t) \times (1 + UAF_t); \\ \text{Target}_t &= \text{Target}_{t-1} \times (1 + SGR_t). \end{aligned}$$

These identities yield

$$UAF_t = \frac{\text{Target}_{t-1} - \text{Actual}_{t-1}}{\text{Actual}_{t-1}} \times 0.75 + \frac{\sum_{t'=1}^{t-2} (\text{Target}_{t'} - \text{Actual}_{t'})}{\text{Actual}_{t-1} \times (1 + SGR_t)} \times 0.33,$$

after being modified by “dampening” weights of 0.75 and 0.33, between components from the previous year and all other years before that, respectively.

The Sustainable Growth Rate (SGR_t) used above is calculated according to four factors: (i) the estimated percentage change in fees for physicians' services, (ii) the estimated percentage change in the average number of Medicare fee-for-service beneficiaries, (iii) the estimated 10-year average annual

percentage change in real gross domestic product per capita, and (iv) the estimated percentage change in expenditures due to changes in law or regulations.

The Budget Neutrality adjustment offsets expenditure changes that result from updates to the relative value units of medical services and ensures that RVU inflation does not change the Medicare budget:

$$BN_t = \frac{\sum_i RVU_{i,t-1} \times q_{i,t-1}}{\sum_i RVU_{i,t} \times q_{i,t-1}},$$

which is closely related to the condition in Equation (A.5.1), in Appendix V, that we use in simulating counterfactual revenue in Section 4.2. Historically, BN_t adjustments have been relatively minor considerations in setting CF_t , compared to MEI_t and UAF_t . Changes to the relative value of medical services via BN_t are also limited by statute to \$20 million annually.

Despite scheduled reductions in the CF according to the SGR formula, the most recent year with a CF reduction was 2002. Since then, Congress has annually overridden scheduled reductions (colloquially known as the “doc fix”). Most recently, the Medicare Access and CHIP Reauthorization Act of 2015 removed the SGR formula used to determine the CF. In its place, the act provided a half-percent increase in the physician fee schedule rate until 2020 (Clough and McClellan, 2016).

II Measuring Affiliation

In economics, several threads of literature have developed quantitative measures of relationships between groups. The literature on segregation has developed measures of isolation and dissimilarity to reflect the interaction between groups (White, 1986; Cutler et al., 1999; Gentzkow and Shapiro, 2011; Esteban et al., 2012). A distinct literature on technological spillovers has sought to measure the likelihood that productive entities in multiple fields may affect each other (Jaffe, 1986; Bloom et al., 2013). In our application, we seek to measure the alignment of interests between specialties when interests are multi-dimensional, and the effects of policies on interests are not known with certainty (Caillaud and Tirole, 2007).

II.A Euclidean Distance Metrics

We capture the multidimensional nature of specialty interests with a measure of *affiliation*, or the alignment of interests between two specialties over a distribution of potential revenue changes across services. We argue in Section 3.3 that using the affiliation formulation instead of service-specific interests alone is attractive for both econometric and conceptual reasons.

Our goal in this section is to rationalize our chosen affiliation measures (in Section 3.3) by showing how we can derive these measures starting from the idea that a specialty’s objective will depend on its total revenue. To account for uncertainty in the effects of price changes on total revenue, we consider a specialty’s total revenue as a stochastic object under random price changes and potentially random spillovers across services. Affiliation is our statistic to measure the degree to which the revenues of two

specialties are linked. Two specialties with linked revenues (i.e., high affiliation) should have similar preferences.

Specifically, starting with the formula for specialty revenue $R_s = \sum_i p_i q_{is}$, we can write the first-order effect of a random vector $d\mathbf{p}$ of price changes on R_s as

$$\frac{dR_s}{d\mathbf{p}} = \sum_i \left(q_{is} \frac{dp_i}{d\mathbf{p}} + p_i \frac{dq_{is}}{d\mathbf{p}} \right). \quad (\text{A.2.1})$$

While we observe q_{is} and p_i , $dp_i/d\mathbf{p}$ and $dq_{is}/d\mathbf{p}$ are generally unknown. Thus, to derive a measure of similarity that captures the effects of $d\mathbf{p}$ on the revenue of two different specialties, as in Equation (A.2.1), we need to make simplifying assumptions on the unknown elements. We discuss two such assumptions below, both of which link a statistical comparison of specialty objectives to a specific measure of affiliation.

II.A.1 Quantity Shares

Under the assumption of fixed quantities (i.e., quantities are completely inelastic to price), the derivative in Equation (A.2.1) reduces to

$$\frac{dR_s}{d\mathbf{p}} = \sum_i q_{is} \frac{dp_i}{d\mathbf{p}}.$$

Further, fixed quantities allow us to scale revenue to be per-service; we can then compare specialties of different overall volume:

$$\frac{dr_s}{d\mathbf{p}} = \sum_i \sigma_{is}^q \frac{dp_i}{d\mathbf{p}},$$

where $r_s \equiv R_s / \sum_i q_{is}$ is the per-service revenue, and $\sigma_{is}^q \equiv q_{is} / \sum_i q_{is}$ is the quantity share of i relative to other procedures that s performs.

The difference in the effect on *per-service revenue* between specialties A and B is

$$\frac{dr_A}{d\mathbf{p}} - \frac{dr_B}{d\mathbf{p}} = \sum_i (\sigma_{iA}^q - \sigma_{iB}^q) \frac{dp_i}{d\mathbf{p}}. \quad (\text{A.2.2})$$

Distances in the vector space of quantity shares, i.e., (σ_A^q, σ_B^q) , thus capture this difference for any arbitrary set of price changes (i.e., any arbitrary \mathbf{p} and the corresponding $dp_i/d\mathbf{p}$ for all i). In addition, the expression in Equation (A.2.2) equivalently represents differences in *per-service profit* due to $d\mathbf{p}$, where “profit” is price minus a concept of service-specific cost, since costs are fixed with fixed quantities.¹ That is, with fixed quantities, a specialty objective that maximizes revenue also maximizes profits.

Given some distribution of price changes $d\mathbf{p}$ with $C \times C$ variance-covariance matrix Ω^q , we can state

¹This cost can be a cost of effort, a financial cost, or an opportunity cost, such as when time used to perform service i detracts from time performing other procedures.

the variance of $dr_A - dr_B$ as

$$\text{Var}(dr_A - dr_B) = (\sigma_A^q - \sigma_B^q)' \Omega^q (\sigma_A^q - \sigma_B^q).$$

Recall that our baseline affiliation metric in Equation (3) is

$$a(s_A, s_B) = -\|\sigma_A^q - \sigma_B^q\|_2 = -\sqrt{(\sigma_A^q - \sigma_B^q)' (\sigma_A^q - \sigma_B^q)}.$$

Here, if two specialties have the same utilization shares (i.e., $\sigma_A^q = \sigma_B^q$), there will be no difference in their per-service revenue (i.e., $dr_A - dr_B = 0$) for any arbitrary distribution of $d\mathbf{p}$. This Euclidean distance is equivalent to the negative standard deviation of $dr_A - dr_B$ under the uninformative prior that $d\mathbf{p}$ follows a distribution with variance-covariance matrix equal to the identity matrix, $\Omega^q = \mathbf{I}_C$. In sum, we can rationalize this affiliation measure if specialties view alignment in interests in terms of per-service revenue, assuming fixed service quantities.

II.A.2 Revenue Shares

Rather than assume fixed quantities as in Appendix II.A.1, we can alternatively assume that quantities remain allocated across specialties in fixed proportion under a distribution of price changes. Under this assumption, we can rationalize a distance metric based on vectors of revenue shares. We show that this metric corresponds to a measure of the difference between two specialties' percentage change in revenue after a distribution of price changes, $d\mathbf{p}$.

To see this, first consider the accounting relationship $q_{is} = w_{is}q_i$, where w_{is} is defined in Equation (5) and $q_i \equiv \sum_s q_{is}$. If we assume that w_{is} is fixed, then a specialty's percentage revenue change is

$$\begin{aligned} \frac{dR_s/d\mathbf{p}}{R_s} &= \frac{1}{R_s} \sum_i \left(q_{is} \frac{dp_i}{d\mathbf{p}} + p_i \frac{dq_{is}}{d\mathbf{p}} \right) \\ &= \sum_i \frac{q_{is} p_i}{R_s} \cdot \frac{q_{is} \cdot dp_i/d\mathbf{p} + p_i \cdot dq_{is}/d\mathbf{p}}{p_i q_{is}} \\ &= \sum_i \sigma_{is}^R \cdot \frac{q_i \cdot dp_i/d\mathbf{p} + p_i \cdot dq_i/d\mathbf{p}}{p_i q_i}, \\ &= \sum_i \sigma_{is}^R \cdot \frac{d(p_i q_i)/d\mathbf{p}}{p_i q_i}, \end{aligned}$$

where $\sigma_{is}^R \equiv (p_i q_{is}) / R_s$ is the revenue share of i relative to other procedures that s performs, and the third line derives from dividing the numerator and the denominator by w_{is} . The term multiplying σ_{is}^R is a constant for each service i ; it does not depend on the identity of s .

The difference in the percentage revenue change between specialties A and B is then

$$\frac{dR_A/d\mathbf{p}}{R_A} - \frac{dR_B/d\mathbf{p}}{R_B} = \sum_i (\sigma_{iA}^R - \sigma_{iB}^R) \frac{d(p_i q_i)/d\mathbf{p}}{p_i q_i}.$$

Distances in the vector space of revenue shares, i.e., $(\sigma_{iA}^R, \sigma_{iB}^R)$, correspondingly capture this difference in percentage revenue changes. Specifically, given some distribution of proportional revenue changes $(p_i q_i)^{-1} d(p_i q_i) / d\mathbf{p}$ distributed with $C \times C$ variance-covariance matrix Ω^R , we can state the variance of the difference in proportional revenue changes between specialties A and B as

$$\text{Var} \left(\frac{dR_A}{R_A} - \frac{dR_B}{R_B} \right) = (\sigma_A^R - \sigma_B^R)' \Omega^R (\sigma_A^R - \sigma_B^R).$$

Thus, the affiliation metric based on revenue shares,

$$a(s_A, s_B) = -\|\sigma_A^R - \sigma_B^R\|_2 = -\sqrt{(\sigma_A^R - \sigma_B^R)' (\sigma_A^R - \sigma_B^R)}, \quad (\text{A.2.3})$$

can be interpreted as the negative standard deviation of the difference in proportional revenue changes (i.e., $dR_A/R_A - dR_B/R_B$) under the uninformative prior that $(p_i q_i)^{-1} d(p_i q_i) / d\mathbf{p}$ is distributed i.i.d. under $\Omega^R = \mathbf{I}_C$. Specialties with identical utilization shares (i.e., $\sigma_A^q = \sigma_B^q$) will also have identical revenue shares (i.e., $\sigma_A^R = \sigma_B^R$) and no difference in proportional revenue changes (i.e., $dR_A/R_A - dR_B/R_B = 0$) regardless of spillovers in Ω^R . In sum, we can rationalize this affiliation measure if specialties view alignment in interests in terms of proportional changes in revenue, and if changes in service quantities are distributed across specialties in fixed proportion.

II.B Alternative Distance Metrics

In addition to affiliation measures detailed above, we consider several other statistical measures of affiliation, motivated by the large space of CPT codes.² First, we modify our baseline Euclidean distance measures by weighting services with greater variation in σ_{is} across s :

$$a(s_A, s_B) = -\sqrt{(\sigma_A - \sigma_B)' \mathbf{G} (\sigma_A - \sigma_B)},$$

where \mathbf{G} is a diagonal weighting matrix, such that element (i, i) is the Gini coefficient across σ_{is} for each service i . This Gini-weighted metric places weight on services with greater variation in σ_{is} and will naturally result in greater variation in distances.

We also consider Manhattan distance, in L_1 space:

$$a(s_A, s_B) = -\|\sigma_A - \sigma_B\|_1 = -\sum_i |\sigma_{iA} - \sigma_{iB}|,$$

²In addition to quantity shares and revenue shares based on individual services defined by CPT codes, we also consider quantity shares and revenue shares in 107 Berenson-Eggers Type of Service (BETOS) categories. This formulation is more restrictive but uses prior knowledge to group services into categories that likely covary. In this sense, this vector space may improve the characterization of affiliation if BETOS categories capture a sufficiently large amount of information about CPT codes in terms of the price or quantity effects of \mathbf{p} . On the other hand, if there remains substantial heterogeneity in effects within BETOS categories, then affiliation measures based on this vector space will perform less well.

Finally, we consider cosine similarity, given by

$$a(s_A, s_B) = \cos(\sigma_A, \sigma_B) = \frac{\sigma_A \cdot \sigma_B}{\sqrt{\sigma_A \cdot \sigma_A} \sqrt{\sigma_B \cdot \sigma_B}}.$$

Cosine similarity—along with related measures of angular distance and the correlation measures in the technology-spillover literature (Jaffe, 1986; Bloom et al., 2013)—has the feature of normalizing the two vectors under comparison to have the same length.³

In this setting, the magnitudes of elements in any vector σ_s represent specialty interests (i.e., $\sum_i \sigma_{is} = 1$ for any s), while normalizing σ_A and σ_B to length 1 has no meaningful economic interpretation. On the other hand, the cosine similarity between two specialty vectors of within-service shares, or w_{is} as defined in Equation (5), can be interpreted as the correlation in revenue between the specialties. To see this, denote $\tilde{\mathbf{w}}_s$ as the $C \times 1$ vector with i th element equal to w_{is} .⁴ Consider a $C \times C$ variance-covariance matrix $\Omega^{w,R}$ of $p_i q_i$. Then $\tilde{\mathbf{w}}_A \Omega^{w,R} \tilde{\mathbf{w}}_B'$ is the covariance in revenues between specialties A and B , under the assumption that $\tilde{\mathbf{w}}_A$ and $\tilde{\mathbf{w}}_B$ are fixed. The measure

$$a(s_A, s_B) = \cos(\tilde{\mathbf{w}}_A, \tilde{\mathbf{w}}_B) = \frac{\tilde{\mathbf{w}}_A \cdot \tilde{\mathbf{w}}_B}{\sqrt{\tilde{\mathbf{w}}_A \cdot \tilde{\mathbf{w}}_A} \sqrt{\tilde{\mathbf{w}}_B \cdot \tilde{\mathbf{w}}_B}} \quad (\text{A.2.4})$$

reflects correlation in revenue between specialties A and B under the uninformative prior that $\Omega^{w,R} = \mathbf{I}_C$. To differentiate $\cos(\sigma_A, \sigma_B)$ and $\cos(\tilde{\mathbf{w}}_A, \tilde{\mathbf{w}}_B)$, we call the former σ -cosine similarity and call the latter w -cosine similarity. In Appendix Table A.3, as with measures based on σ_{is} , we also present regression results of Equation (6) for affiliation defined by w -cosine similarity measures based on quantity and revenue data.⁵

II.C Cross-Service Spillovers

In Appendices II.A and II.B, we describe affiliation measures that assume revenue-relevant variation is i.i.d. across services. Here, we empirically compute and evaluate alternative variance-covariance matrices to represent spillovers. We compute three different matrices relevant for three respective affiliation measures: (i) Ω^q , the variance-covariance matrix of RVU changes dp_i , implicit in Equation (3); (ii) Ω^R , the variance-covariance matrix of percentage revenue changes $d(p_i q_i) / (p_i q_i)$, implicit in Equation (A.2.3); and (iii) $\Omega^{w,R}$, the variance-covariance matrix of revenue $d(p_i q_i)$, implicit in Equation (A.2.4).

³To see the relationship between between Euclidean distance and cosine similarity, note that $\|\sigma_A - \sigma_B\|_2^2 = (\sigma_A - \sigma_B)(\sigma_A - \sigma_B)' = \|\sigma_A\|_2^2 + \|\sigma_B\|_2^2 - 2\sigma_A \cdot \sigma_B$. If $\|\sigma_A\|_2^2 = \|\sigma_B\|_2^2 = 1$, then $\|\sigma_A - \sigma_B\|_2^2 = 2(1 - \cos(\sigma_A, \sigma_B))$. Angular distance is defined as $a(s_A, s_B) = \pi^{-1} \cos^{-1}(\cos(\sigma_A, \sigma_B))$, and correlation is defined as $a(s_A, s_B) = \text{corr}(\sigma_A, \sigma_B)$. We find that regressions of Equation (6) yield very similar results when using cosine similarity, angular distance, and correlation. We thus omit results for angular distance and correlation from Appendix Table A.3 for brevity.

⁴This vector is related to \mathbf{w}_i , which is the $S \times 1$ vector with the s th element equal to w_{is} .

⁵Quantity-based w_{is}^q is defined in Equation (5), whereas revenue-based $w_{is}^R = (\sum_y p_{iy} q_{isy}) / (\sum_y \sum_s p_{iy} q_{isy})$. For a single year y , it is obvious that $w_{is}^q = w_{is}^R$. In general, they may not be equivalent when aggregating over years or CPT codes within a BETOS category, but the difference between w_{is}^q and w_{is}^R will be much smaller than the difference between σ_{is}^q and σ_{is}^R , because price differences are much smaller within CPT code as opposed to across CPT codes.

We compute these matrices based on observations of p_i in the physician fee schedule and $p_i q_i$ across years in the Medicare data.

The assumptions about cross-service spillovers in each of these matrices will imply different affiliation measures. Specifically, we define

$$\begin{aligned} -\|\sigma_A^q - \sigma_B^q; \Omega^q\|_2 &= -\sqrt{(\sigma_A^q - \sigma_B^q)' \Omega^q (\sigma_A^q - \sigma_B^q)}; \\ -\|\sigma_A^R - \sigma_B^R; \Omega^R\|_2 &= -\sqrt{(\sigma_A^R - \sigma_B^R)' \Omega^R (\sigma_A^R - \sigma_B^R)}; \\ \cos(\tilde{\mathbf{w}}_A, \tilde{\mathbf{w}}_B; \Omega^{w,R}) &= \frac{\tilde{\mathbf{w}}_A \Omega^{w,R} \tilde{\mathbf{w}}_B'}{\sqrt{\tilde{\mathbf{w}}_A \Omega^{w,R} \tilde{\mathbf{w}}_A'} \sqrt{\tilde{\mathbf{w}}_B \Omega^{w,R} \tilde{\mathbf{w}}_B'}} \end{aligned}$$

for Euclidean distance in σ^q , Euclidean distance in σ^R , and w -cosine similarity, respectively.

In principle, if spillovers are known without measurement error, these affiliation measures should capture the alignment of specialty revenue interests more closely than a measure that ignores spillovers. However, in practice, there are two empirical difficulties that could degrade the fidelity of these measures relative to our baseline measure. First, we lack sufficient quasi-experimental variation to estimate spillovers across services. Second, the number of observations we have for each service is much smaller than the number of elements in Ω , a well-known problem in the estimation of covariance structures (Altonji and Segal, 1996).

Thus, we introduce two regularization parameters, γ_1 and γ_2 , to enable us to “shrink” the variance-covariance matrix Ω to a matrix $\Omega_{\gamma_1, \gamma_2}$ closer to the identity matrix \mathbf{I}_C :

$$\begin{aligned} \Omega_{\gamma_1, 0} &= (\text{diag}(\Omega))^{-\gamma_1/2} \Omega (\text{diag}(\Omega))^{-\gamma_1/2} \\ \Omega_{\gamma_1, \gamma_2}[i, j] &= (1 - \gamma_2) \Omega_{\gamma_1, 0}[i, j], \text{ for all } i \neq j. \end{aligned}$$

$\gamma_1 \in [0, 1]$ transforms $\Omega_{\gamma_1, 0}$ from a variance-covariance matrix ($\gamma_1 = 0$) to a correlation matrix ($\gamma_1 = 1$), and $\gamma_2 \in [0, 1]$ further transforms Ω_{1, γ_2} from a correlation matrix ($\gamma_2 = 0$) to an identity matrix ($\gamma_2 = 1$).

In Appendix Figure A.1, we evaluate the performance of affiliation metrics that include spillovers, by plotting the coefficient of each affiliation metric in the price regression of Equation (6) with respect to the regularization parameters. We find that accounting for spillovers unambiguously reduces the linkage between RUC price actions and our Euclidean-distance affiliation measures but improves this linkage for w -cosine similarity over some range of (γ_1, γ_2) .

III Mixed Strategies in Endogenous Proposals

In this appendix, we sketch a simple signaling model of proposals to provide intuition for the random variation we observe in the endogenous decisions of specialties to propose. As in our main conceptual framework, in Section 5.1, we assume a specialty society may be biased, but for tractability, we rule out

any downstream communication or any potential bias of the RUC.⁶ The first important feature of the model is that proposals to the RUC are costly. Second, if there is more than one proposing specialty that would have proposed alone, then there cannot be a unique (or symmetric) pure strategy equilibrium that determines specialty proposals. In other words, if specialty societies cannot fully coordinate, then we will have random variation in the identities of proposing specialties. In this sketch, we ignore the possibility that costs may quasi-randomly vary in order to clarify the latter source of random variation.

Specifically, consider specialty society utility

$$u_S = -(\theta + b_S - p)^2 - cD_S,$$

where $\theta \in \{0, 1\}$ is the true price, $b_S > 0$ is the specialty's bias, p is the price recommended by the RUC (and set by the government), c is the cost of proposing, and $D_S \in \{0, 1\}$ is an indicator for the specialty proposing. The RUC's (and the government's) utility is $u_R = -(\theta - p)^2$. We assume that $\Pr(\theta = 1) = \frac{1}{2}$.

In a separating pure strategy equilibrium with a single specialty, the specialty will propose if and only if $\theta = 1$, and the government will set $p = D_S$. The specialty must then have bias $b_S \in \left[\frac{c-1}{2}, \frac{c+1}{2}\right]$. If bias is too low (or cost too high), then the specialty will not want to propose even if $\theta = 1$; if bias is too high (or cost too low), then the specialty will want to propose even if $\theta = 0$.⁷

We then consider two specialties $S \in \{1, 2\}$, and assume that $b_S > \frac{c-1}{2}$ for both specialties. Both specialties would propose if $\theta = 1$ had the other one not existed, yet neither would propose if it knows that the other specialty's strategy is to propose when $\theta = 1$. Thus, there is no unique pure strategy equilibrium of proposals by the two specialties. In the case that $b_1 = b_2$, this implies that there is no symmetric pure strategy equilibrium.⁸ There are at least two types of mixed strategies over the range of this bias-cost space: (i) Neither specialty proposes if $\theta = 0$ and mix (i.e., propose with some probability $\pi_S \in (0, 1)$) if $\theta = 1$, and (ii) both specialties propose if $\theta = 1$ and mix if $\theta = 0$.

Because the number of actual specialty-proposals relative to potential specialty-proposals is empirically low, we focus on the former type of mixed strategies.⁹ When specialties mix when $\theta = 1$, the RUC knows that $\theta = 1$ and sets $p = 1$, if either $D_1 = 1$ or $D_2 = 1$. If $D_1 = D_2 = 0$, the RUC sets

$$p(\pi_1, \pi_2 | D_1 = D_2 = 0) = \frac{(1 - \pi_1)(1 - \pi_2)}{1 + (1 - \pi_1)(1 - \pi_2)},$$

which is the probability that $\theta = 1$ if $D_1 = D_2 = 0$. For a mixed-strategy equilibrium to exist, specialties must be indifferent between proposing and not. Specifically, although proposing will lead to a price

⁶We could introduce these features, but the intuition we wish to formalize would remain the same.

⁷Potters and van Winden (1992) also point out that there exists a mixed strategy equilibrium, in which the specialty certainly proposes if $\theta = 1$ and proposes with some probability $\pi \in (0, 1)$ if $\theta = 0$ for biases $b_S \in \left(\frac{c+1}{2}, c + \frac{1}{4}\right)$ if $c > \frac{1}{2}$.

⁸There may exist, for example, a perfect Bayesian equilibrium with two players in which both would choose to propose if the RUC believed $\theta = 1$ only if it observes both specialties proposing. We could rule out an equilibrium of this form by refining the equilibrium concept such that if the RUC observes only one specialty proposing, it will nonetheless consider that specialty's incentives to propose and update its prior probability that the value of $\theta = 1$ (Grossman and Helpman, 2001).

⁹Parallel results obtain for the latter type, which correspond to the mixed strategy in the single-player case noted by Potters and van Winden (1992), in footnote 7.

increase of $1 - p(\pi_1, \pi_2 | D_1 = D_2 = 0) > 0$, the utility gain by either specialty is equal to the cost of proposing, c . In Appendix Figure A.2, fixing $c = 1$ for the specialties, we show whether a mixed-strategy equilibrium exists in (b_1, b_2) space and, if so, the mixing probabilities for the specialties (when $\theta = 1$) that sustain it.

We first find that if specialty bias is sufficiently low, then there exists no mixed-strategy equilibrium. Failure to coordinate and the temptation to free-ride results in no proposals, reducing signaling equilibria relative to the one-specialty standard. However, if both specialties are sufficiently biased (or equivalently, have low costs), then their equilibrium mixed strategies will involve fairly high π_S , and signaling is possible even for $b_S > \frac{c+1}{2}$, which would have prohibited signaling in the one-specialty case, where the specialty would have proposed even if $\theta = 0$. Finally, and intuitively, when specialty are asymmetric in their bias, signaling occurs mostly through the lower-bias specialty. As the bias of the higher-bias specialty approaches infinity, the equilibrium resembles a single-specialty pure-strategy equilibrium, and signaling is possible at levels of bias (of the lower-bias specialty) close to those in the one-specialty case (i.e., as low as $\frac{c-1}{2}$).

IV Quasi-Experimental Variation in Affiliation

Affiliation $A(\mathcal{R}_t, \mathcal{S}_i)$ is determined as a function of specialties on the RUC at meeting t , \mathcal{R}_t , and specialties on a proposal i , \mathcal{S}_i . In this appendix, we quantify and assess the exogeneity of variation in $A(\mathcal{R}_t, \mathcal{S}_i)$ due to variation in \mathcal{R}_t and variation in \mathcal{S}_i . In particular, we evaluate two potential threats to identification. First, with respect to variation in \mathcal{R}_t , specialties submitting proposals for procedures with intrinsically high prices may choose to submit these proposals at meetings with more affiliated RUC members. Second, specialties may be more likely to propose for procedures with higher potential prices, driving up the affiliation of these proposals with the RUC.

IV.A Quasi-Experimental Variation in \mathcal{R}_t

To evaluate variation in affiliation due to \mathcal{R}_t we first compute the affiliation that each proposal i would have over all possible meetings $t' \in T$, generating a set of counterfactual affiliations, $A = \{A(\mathcal{R}_{t'}, \mathcal{S}_i)\}$. We then test whether observed affiliations are statistically distinguishable from these counterfactual affiliations. In Panel A of Appendix Figure A.4, we show that the mean differenced statistic $A(\mathcal{R}_{t'}, \mathcal{S}_i) - A(\mathcal{R}_t, \mathcal{S}_i)$ over all proposals and possible meeting dates (i, t') is not statistically different than 0. However, given relatively stable RUC specialty membership in Table I and Figure I, it is natural that the variation in affiliation due to \mathcal{R}_t is relatively small. If we restrict counterfactual meetings to those within a year of the actual meeting, in Panel B, we find that the distribution of $A(\mathcal{R}_{t'}, \mathcal{S}_i) - A(\mathcal{R}_t, \mathcal{S}_i)$ is even more concentrated around zero.

We can also quantify the variation component from \mathcal{R}_t relative to overall quasi-experimental variation. For this decomposition, we compute $\bar{A}(\mathcal{S}_i) \equiv \|T\|^{-1} \sum_{t' \in T} A(\mathcal{R}_{t'}, \mathcal{S}_i)$, which is the average variation across all meetings, given \mathcal{S}_i . We then compute the variation in $\bar{A}(\mathcal{S}_i)$, conditional on \mathbf{w}_i ; we

denote $\bar{A}(\mathcal{S}_i)$ residualized by \mathbf{w}_i as $\bar{A}^*(\mathcal{S}_i)$. Variation in $\bar{A}^*(\mathcal{S}_i)$ represents quasi-experimental variation unrelated to \mathbf{w}_i . The component of the variation due to \mathcal{R}_t is $\sigma_{\mathcal{R}}^2 \equiv \text{Var}(A(\mathcal{R}_t, \mathcal{S}_i) - \bar{A}(\mathcal{S}_i))$, and the remaining component due to \mathcal{S}_i is $\sigma_{\mathcal{S}}^2 \equiv \text{Var}(\bar{A}^*(\mathcal{S}_i))$. We find that $\sigma_{\mathcal{R}}^2 / (\sigma_{\mathcal{R}}^2 + \sigma_{\mathcal{S}}^2) \approx 0.014$ when T is the entire set of meetings, and $\sigma_{\mathcal{R}}^2 / (\sigma_{\mathcal{R}}^2 + \sigma_{\mathcal{S}}^2) \approx 0.007$ when T contains counterfactual meetings at most three meetings (one year) apart from the actual meeting.

IV.B Quasi-Experimental Variation in \mathcal{S}_i

To assess quasi-experimental variation in \mathcal{S}_i empirically, we conduct four tests. First, we show that specialty participation in proposals, conditional on specialty dummies, meeting dummies \mathbf{T}_t , and utilization shares \mathbf{w}_i , is uncorrelated with the service’s predicted price. Second, we show that specialty proposals are conditionally uncorrelated with time-varying affiliation with the RUC. Third, we show significant variation in the propensity of specialty proposals, even among specialties that actually participate in a given proposal. Fourth, we predict affiliation based on specialty-proposal propensities and show that this prediction is forecast-unbiased (Chetty et al., 2014), while there also remains wide variation in the distribution of actual minus predicted affiliation. We provide more detail on these tests below.

IV.B.1 Specialty-Proposal Probability

The first three tests we perform relate to specialty-proposal probabilities. First, in Appendix Figure A.5, we show evidence that the probability a specialty participates in a proposal is conditionally uncorrelated with the predicted price of the relevant service. We predict the RVU of a procedure by its characteristics, including procedure code word descriptions, surveyed time, prior RVU, and Medicare beneficiary characteristics, which yields an adjusted R^2 of 0.88 for the RVU prediction equation. Controlling for specialty dummies, meeting dummies \mathbf{T}_t , and specialty utilization shares $w_{i,s}$, as defined in Equation (5), we find no significant relationship between specialty proposals and predictors of price.

Second, in Appendix Figure A.6, we assess whether specialty proposals are more likely when affiliation with the RUC is higher. We construct a measure of whether affiliation between specialty s is higher at meeting $t(i)$ associated with proposal i than at other meetings

$$A(\mathcal{R}_{t(i), s}) - \bar{A}(s),$$

where $\bar{A}(s) \equiv \|T\|^{-1} \sum_{t' \in T} A(\mathcal{R}_{t'}, s)$. We standardize $A(\mathcal{R}_{t(i), s}) - \bar{A}(s)$ to have a distribution with mean 0 and standard deviation 1. We then evaluate whether specialty proposals, or $\mathbf{1}(s \in \mathcal{S}_i)$, is correlated with $A(\mathcal{R}_{t(i), s}) - \bar{A}(s)$, conditional on dummies for specialty s and for the number of proposing specialties in \mathcal{S}_i , or $\|\mathcal{S}_i\|$. We again find no significant relationship between time-varying affiliation between s and $\mathcal{R}_{t(i)}$ and whether $s \in \mathcal{S}_i$. While this does not rule out strategic proposing with respect to affiliation that is *time-invariant*, given the evidence in Appendix IV.A, it is intuitive that specialties do not have much scope to respond to time-varying affiliation.

Third, we form a prediction of specialty-proposal propensities, in order to evaluate variation in this

propensity and the predictability with which specialties actually propose. We estimate a logit propensity model of specialty-proposal participation, using specialty identities, flexible functions of \mathbf{w}_i , and the procedure’s share of specialty revenue, defined as σ_{is}^R in Appendix II.A.2. The logit model is fairly predictive, with a pseudo- R^2 of 0.73 and a log-likelihood of $-8,661.35$ over 248,735 observations, and the standard deviation in specialty-proposal propensities is about 13%. Nonetheless, we find substantial residual variation in specialty proposals. To illustrate this, in Appendix Figure A.7, we show the propensities of 6,929 actual specialty-proposal pairs over 4,199 proposals. While there are many propensities with high values, more than half of the actual specialty proposals have propensities lower than 0.8, and about a quarter have propensities less than 0.5. Similarly, in Appendix Figure A.8, we show the first-, second-, third-, and fourth-ranked specialty propensities for proposals *with at least as many proposers*. Although there are 64 specialties to rank, propensities quickly diminish: The average first-ranked propensity is 0.86, while the average second-, third-, and fourth-ranked propensities are 0.76, 0.69, and 0.54, respectively.

IV.B.2 Affiliation Forecast

In our fourth test, we use our estimated specialty-proposal propensities, $\hat{\pi}_{is}$, and the known specialties of RUC members at each meeting, \mathcal{R}_t , to form a prediction of affiliation by simulation. We will use this prediction to evaluate endogeneity at the affiliation level, testing whether affiliation is “forecast-unbiased” (Chetty et al., 2014). We will also evaluate the degree of variation in affiliation that remains conditional on this prediction, which allows for nonlinear relationships in \mathbf{w}_i and σ_{is}^R across specialties.

We proceed as follows:

1. Use estimated specialty-proposal propensities, $\hat{\pi}_{is}$. Drop any specialty-proposal pair with $\hat{\pi}_{is} < 0.01$.
2. For each proposal i , identify number of remaining specialty-proposer candidates, n_i , and the number of actual specialty proposers, k_i . This yields $\|\mathbb{S}_i\| = C(n_i, k_i)$ as the number of potential proposer sets \mathcal{S}_i for i , constraining the number of simulated proposers in each set to be the same as the number of actual proposers. For example, if there remain ten specialty-proposer candidates for a proposal with only one actual specialty proposer, there are $C(10, 1) = 10$ (singleton) sets to draw from. However, if there are fifteen specialty-proposer candidates for a proposal with four actual proposers, there are $C(15, 4) \approx 7.57 \times 10^7$ sets to draw from.
 - (a) For proposals i such that $\|\mathbb{S}_i\| \leq 50$, collect all such potential proposer sets.
 - (b) For the remaining proposals, randomly draw k_i proposers from n_i , oversampling specialty-proposer candidates from those with higher $\hat{\pi}_{is}$. Specifically, generate $r_{is} \sim U(0, 1)$ and subtract this from $\hat{\pi}_{is}$. Within each i , sort specialty-proposer candidates by $\hat{\pi}_{is} - r_{is}$, and choose the top k_i candidates to include in \mathcal{S}_i . Repeat until some stopping rule (e.g., based on the number of unique sets sampled for each i and the lack of new sets sampled for any i in a draw).

(c) Denote as $\mathbb{S}_i^* \subseteq \mathbb{S}_i$ the collection of simulated sets for each proposal i . For each $\mathcal{S}_i \in \mathbb{S}_i^*$, calculate a simulated set affiliation $A(\mathcal{R}_t, \mathcal{S}_i)$ for each \mathcal{S}_i , using known \mathcal{R}_t and the formula in Equation (4).

3. Given $\hat{\pi}_{i,s}$, and assuming independence of specialty proposals, the probability of drawing \mathcal{S}_i from \mathbb{S}_i is

$$\Pr(\mathcal{S}_i | \mathbb{S}_i^*) \equiv \frac{\prod_{s \in \mathcal{S}_i} \hat{\pi}_{i,s} \prod_{s \notin \mathcal{S}_i} (1 - \hat{\pi}_{i,s})}{\sum_{\mathcal{S}_i \in \mathbb{S}_i^*} \left(\prod_{s \in \mathcal{S}_i} \hat{\pi}_{i,s} \prod_{s \notin \mathcal{S}_i} (1 - \hat{\pi}_{i,s}) \right)}.$$

This allows us to weight sets by their probability of occurrence. This also allows us to generate a *predicted* set affiliation,

$$\hat{A}(\mathcal{R}_t, i) = \sum_{\mathcal{S}_i \in \mathbb{S}_i^*} A(\mathcal{R}_t, \mathcal{S}_i) \Pr(\mathcal{S}_i | \mathbb{S}_i^*). \quad (\text{A.4.1})$$

In Appendix Figure A.9, we show the distribution of simulated set affiliations relative to the actual set affiliation for each i , weighted by $\Pr(\mathcal{S}_i | \mathbb{S}_i^*)$, or $\hat{A}(\mathcal{R}_t, i) - A(\mathcal{R}_t, \mathcal{S}_i)$. The weighted standard deviation of the distribution is 0.242, reflecting that there exists meaningful variation in set affiliation based on the specialty-proposal propensities. The variation in this figure is much larger than the variation in Appendix Figure A.6, consistent with the large majority of identifying variation coming from \mathcal{S}_i rather than \mathcal{R}_t . Further, the weighted mean of the distribution of $\hat{A}(\mathcal{R}_t, i) - A(\mathcal{R}_t, \mathcal{S}_i)$ is -0.016 , suggesting very little forecast bias in predicted set affiliation. We use predicted set affiliation as a control, rather than linear specialty shares of CPT utilization, \mathbf{w}_i , in a robustness check of the affiliation effect on prices, in column (5) of Table III; we find a similar estimate of the main effect.

V Counterfactual Revenue Analysis

V.A Simulation Algorithm

We simulate counterfactual revenue in scenarios that entail counterfactual affiliations for proposals. In each scenario, we hold fixed the service and timing of each proposal, the Medicare budget, and the utilization of each service. Counterfactual revenue results solely from the effect of affiliation on relative price. Prices are rationalized so that total spending meets the fixed Medicare budget. The algorithm is as follows:

1. Starting at the first year in which the RUC's pricing decision goes into effect, we replace the relative price RVU_{iy} that followed a RUC recommendation with a counterfactual \widetilde{RVU}_{iy} , by subtracting $\hat{\alpha} \left(A(\mathcal{R}_t, \mathcal{S}_i) - \tilde{A}_{it} \right)$, where $A(\mathcal{R}_t, \mathcal{S}_i)$ and \tilde{A}_{it} are actual and counterfactual affiliations, respectively, and $\hat{\alpha}$ is the estimated affiliation effect from Equation (6). The counterfactual affiliation in the first scenario is an equalized affiliation across all proposals $i \in I_t$ in the same meeting t : $\tilde{A}_{it} = \|I_t\|^{-1} \sum_{i \in I_t} A(\mathcal{R}_t, \mathcal{S}_i)$. The counterfactual affiliation in the second scenario is $\tilde{A}_{it} = A(\tilde{\mathcal{R}}, \mathcal{S}_i)$, where $\tilde{\mathcal{R}}$ is the counterfactual RUC composed of specialties in Appendix Table

A.7. RUC decisions in meeting t map to prices in the Medicare schedule in year $y(t)$. We repeat for subsequent years, allowing previously set prices to continue forward.

2. We take quantities q_{isy} of service i , by specialty s , in year y , observed in Medicare claims. We set conversion factors CF_y and \widetilde{CF}_y so that the overall spending is \$70 billion in 2014 dollars, which implies that

$$\widetilde{CF}_y \sum_i \sum_s \widetilde{RVU}_{iy} \cdot q_{isy} = CF_y \sum_i \sum_s RVU_{iy} \cdot q_{isy}. \quad (\text{A.5.1})$$

3. The revenue reallocation for service i , specialty s , and year y is

$$\Delta r_{isy} = q_{isy} \left(\widetilde{CF}_y \cdot \widetilde{RVU}_{iy} - CF_y \cdot RVU_{iy} \right).$$

4. We aggregate Δr_{isy} to yearly averages for specialties s or types of service k :

$$\begin{aligned} \Delta R_s &= \|\mathcal{Y}\|^{-1} \sum_{y \in \mathcal{Y}} \sum_i \Delta r_{isy}; \\ \Delta R_k &= \|\mathcal{Y}\|^{-1} \sum_{y \in \mathcal{Y}} \sum_s \sum_{i \in k} \Delta r_{isy}. \end{aligned}$$

V.B Distribution of Counterfactual Affiliations

Our counterfactual analysis is based on a reduced-form estimate of $\hat{\alpha}$ from Equation (6). In the first counterfactual scenario, we assume that affiliation has no effect, or that there is no difference in affiliation across proposals in a given meeting. In the second counterfactual scenario, we consider an alternative RUC membership, and use $\hat{\alpha}$ to impute counterfactual RVUs, as described above. To evaluate the external validity of using $\hat{\alpha}$ in this analysis, we compare the distribution of counterfactual affiliations under this alternative RUC with the observed distribution of actual affiliations.

In Appendix Figure A.11, we plot the distribution of counterfactual affiliations against that of actual affiliations and find very little difference between the two distributions. The Q-Q plot of quantiles of the two distribution essentially lie on the 45-degree line. In the same figure, we also consider the distribution of differences between counterfactual and actual affiliation. This distribution is quite narrow, especially compared to the distribution of the difference between actual and predicted affiliation. Thus, the differences in affiliation induced by a counterfactual RUC appear quite small relative to the quasi-experimental variation in affiliation we observe in the data.

VI Alternative Mechanisms Behind the Price Effect

In this appendix, we consider evidence regarding alternative mechanisms of the affiliation effect on prices, as discussed in Section 4.3. The results are summarized in Appendix Table A.4. All specifications in Appendix Table A.4 include the same controls as in the baseline specification of the price regression,

shown in column (4) of Table III.

First, we consider specifications relating to interests (and information) held by RUC specialties that are specific to the proposed service. Specifically, we consider the service i 's utilization share of all services billed by a RUC specialty s , or σ_{is}^q , as defined in Equation (2). We also consider i 's revenue share of all Medicare revenue to s , or $\sigma_{is}^R \equiv (p_i q_{is}) / R_s$, as discussed in Appendix II.A.2. These measures capture both specialty s 's interests and information about i : A specialty s with a higher σ_{is}^q or σ_{is}^R should have interests specific to service i to raise its price, and it may also have more knowledge about service i , outside of the proposal process. We perform variants of the regression

$$\ln \text{RVU}_{it} = \alpha A(\mathcal{R}_t, \mathcal{S}_i) + \gamma m(\sigma_i; \mathcal{R}_t) + \mathbf{X}_i \beta + \mathbf{T}_t \eta + \mathbf{w}_i \zeta + \varepsilon_{it}, \quad (\text{A.6.1})$$

where $m(\sigma_i; \mathcal{R}_t)$ is the mean interest σ_{is} across specialties serving on the RUC, $s \in \mathcal{R}_t$, standardized to have mean 0 and standard deviation 1 across i .¹⁰

Columns (1) and (2) of Appendix Table A.4 show results for regressions adding standardized mean σ_{is}^q and σ_{is}^R , respectively. The coefficient on standardized set affiliation remains unchanged in magnitude and significance. The coefficients on the standardized measures of RUC-specialty interest in proposal i are small, though statistically significant. Although we ascribe a causal interpretation to α under Assumption 1 in Section 3.4, the same reasoning does not apply to γ .¹¹ With this caveat, it does not appear that RUC specialty direct interests play a major role in explaining the RUC's price recommendations. In columns (3) and (4), we consider related interests, or elements $\tilde{\sigma}_{is}^q$ and $\tilde{\sigma}_{is}^R$ in vectors $\tilde{\sigma}_s^q = \Omega^q \sigma_s^q$ and $\tilde{\sigma}_s^R = \Omega^R \sigma_s^R$, respectively, where Ω^q and Ω^R are spillover matrices defined in Appendix II.C. Interestingly, we find that related interests play a larger role in pricing than direct interests.

Next, we consider the possibility that affiliation could reflect signaling “buy-in.” That is, more specialties should be willing to propose for procedures that have a higher intrinsic price. As more specialties propose, set affiliation, as defined in Equation (4), will mechanically increase through max operator in the formula. Higher prices under this scenario are warranted and do not reflect any RUC bias. We modify the baseline price-effect regression in Equation (6) to include proposer-count fixed effects:

$$\ln \text{RVU}_{it} = \alpha A(\mathcal{R}_t, \mathcal{S}_i) + \gamma_n \mathbf{1}(\|\mathcal{S}_i\| = n) + \mathbf{X}_i \beta + \mathbf{T}_t \eta + \mathbf{w}_i \zeta + \varepsilon_{it}. \quad (\text{A.6.2})$$

This specification relies only on within-proposer-count variation to identify the price effect of affiliation. As shown in column (5) of Appendix Table A.4, the coefficient on standardized set affiliation is unchanged, at 0.112, and highly significant.

¹⁰We also perform a regression similar to Equation A.6.1, excluding the term $A(\mathcal{R}_t, \mathcal{S}_i)$, which also yields similar estimates of γ (omitted for brevity). This indicates that $m(\sigma_i; \mathcal{R}_t)$ is for the most part conditionally uncorrelated with $A(\mathcal{R}_t, \mathcal{S}_i)$.

¹¹For nonparametric identification of γ , we would require random variation in RUC specialty composition, \mathcal{R}_t . In order to interpret γ as causal, we would require parametric restrictions on the conditional independence between $\ln \text{RVU}_{it}$ and $m(\sigma_i; \mathcal{R}_t)$ —such as the sufficiency of conditioning on the linear combination $\mathbf{w}_i \zeta$ and $\ln \sum_s q_{is}$. While the causal interpretation of γ is not important for this paper, we conduct balance tests similar to the test that generates Appendix Figure A.3, which generally reject the null of quasi-random assignment, even when we control for $\ln \sum_s q_{is}$.

VII Heterogeneous Effect of Affiliation by Proposal Type

We investigate heterogeneity of the affiliation effect on prices, along four binary dimensions of proposal type: (i) whether the proposal is for a CPT code that existed or was new at the time of the proposal, (ii) whether the proposal is for a CPT code with below- or above-median yearly volume (for the years that it was in existence), (iii) whether the proposal is for a CPT code with below- or above-median price, and (iv) whether the proposal occurred at an earlier or later RUC meeting.¹² For each of these dimensions, we perform the following regression:

$$\ln \text{RVU}_{it} = \sum_{c \in \{0,1\}} (\alpha_{0,c} + \alpha_{1,c} A(\mathcal{R}_t, \mathcal{S}_i)) \cdot \mathbf{1}(c(i,t) = c) + \mathbf{X}_i \beta + \mathbf{T}_t \eta + \mathbf{w}_i \zeta + \varepsilon_{it}, \quad (\text{A.7.1})$$

where $c(i,t) \in \{0,1\}$ depending on CPT code i and meeting t in question.

Appendix Table A.5 shows cross-tabulations of proposals along these types. Approximately 55% of the proposals were for existing CPT codes, while the remaining 45% were for new CPT codes. Existing CPT codes were slightly more likely to have above-median utilization volumes, and much more likely to have above-median prices. High-priced CPT codes were slightly more likely to have higher volumes.

Appendix Table A.6 shows results of the regression in Equation (A.7.1), along each of the four dimensions. Strikingly, nearly all of the effect of affiliation on prices is borne by proposals for new CPT codes. The coefficient on (interacted) set affiliation is twice as high for new CPT codes, at 0.209, while it is small and statistically insignificant for existing CPT codes. The effect of affiliation is also much higher for low-quantity vs. high-quantity CPT codes, and it is much higher for low-priced vs. high-priced CPT codes. Finally, the effect of affiliation is roughly the same in earlier meetings as it is in later meetings. Because proposal types are correlated across dimensions, these heterogeneous treatment effects are only descriptive. However, they are consistent with a story in which affiliation has a greater relative effect for proposals in which there is less evidence (i.e., less hard information) or less at stake for setting a service’s price.

VIII Technical Details of the Conceptual Framework

This appendix provides additional detail behind the conceptual framework we outline in Section 5. We start with more detail about the formula for expected “variance”, $E[(\theta + b_R - p)^2]$, that represents information loss in the standard Crawford and Sobel (1982) model. Next, we provide details of the analysis with hard information and the optimal b_R^* under hard information. Finally, we describe a mechanism of

¹²Although price is endogenous, when considered as an indicator variable for whether the CPT code’s price is below- or above-median, we roughly capture intrinsic characteristics of the procedure. For example, the highest-priced CPT code (CPT code 33935, or heart and lung transplantation) has an RVU of 100, 670 CPT codes have RVUs below 1. The mean RVU was 10.85, and the median RVU was 5.53, shared by CPT 22585 (Anterior or Anterolateral Approach Technique Arthrodesis Procedures on the Spine) and CPT code 33213 (Pacemaker or Pacing Cardioverter-Defibrillator Procedures). We define an “earlier” meeting as occurring before the third meeting of 2005, whereas a “later” meeting occurred at or after the third meeting of 2005.

assigning intervals of *expected* length L such that the posterior distribution of θ remains uniform within each realized interval.

VIII.A Canonical Crawford and Sobel (1982) Partitions

Consider θ uniformly distributed on the interval $[0, L]$. The sender (the specialty) has bias b , relative to the receiver (the RUC). The formula for the number of partitions supported under $b = b_S - b_R$ over the interval is

$$n^*(b) = \left\lfloor \frac{1}{2} \left(1 + \sqrt{1 + \frac{2L}{b}} \right) \right\rfloor. \quad (\text{A.8.1})$$

Using Equation (A.8.1), we define the limiting bias such that $n^*(b - \varepsilon) = n$ for any positive but arbitrarily small ε :

$$b^*(n) = \frac{2L}{(2n-1)^2 - 1}.$$

$b^*(n)$ supports n partitions only in the limit. For example, as we show below, $b = \frac{1}{4}$ supports only one partition, since the first partition of technically two partitions will have a length of 0.

The first partition is bounded by $x_0 = 0$ and

$$x_1 = \frac{L}{n} - (n-1)2b, \quad (\text{A.8.2})$$

Subsequent partition lengths increase by $4b$, which implies

$$x_k = 2x_{k-1} - x_{k-2} + 4b, \quad (\text{A.8.3})$$

and Equations (A.8.2) and (A.8.3) imply that $x_n = L$.

We will consider a number of specific examples of n , which exist for $b \in [b^*(n+1), b^*(n))$. We define the boundaries of the partitions in the space of $[0, L]$, and the variance $E[(\theta + b_R - p)^2]$. For the latter object, we use the fact that the variance of a uniformly distributed random variable along an interval of length L is $L^2/12$. Two partitions exist if $b \in [\frac{L}{12}, \frac{L}{4})$ and are defined by $(0, \frac{L}{2} - 2b, L)$. The variance is given by

$$\begin{aligned} E[(\theta + b_R - p)^2] &= \frac{L^2}{12} \left[\left(\frac{1}{2} - 2b \right)^3 + \left(\frac{1}{2} + 2b \right)^3 \right] \\ &= \frac{1}{12} \left(\frac{L^2}{4} + 12b^2 \right) = \frac{L^2}{48} + b^2. \end{aligned}$$

Three partitions exist if $b \in \left[\frac{L}{24}, \frac{L}{12}\right)$ and are defined by $\left(0, \frac{L}{3} - 4b, \frac{2L}{3} - 4b, L\right)$. The variance is given by

$$\begin{aligned} E[(\theta + b_R - p)^2] &= \frac{L^2}{12} \left[\left(\frac{1}{3} - \frac{4b}{L}\right)^3 + \left(\frac{1}{3}\right)^3 + \left(\frac{1}{3} + \frac{4b}{L}\right)^3 \right] \\ &= \frac{1}{12} \left(\frac{L^2}{9} + 32b^2 \right). \end{aligned}$$

By induction, one can verify that the variance in the equilibrium with n partitions is

$$E[(\theta + b_R - p)^2] = \frac{1}{12} \left(\frac{L^2}{n^2} + A_n b^2 \right), \quad (\text{A.8.4})$$

where $A_1 = 0$, and $A_n = A_{n-1} + 8n - 4$. Note that the variance is continuous across the number of partitions (as b changes). Also, the variance is decreasing in b , holding L fixed.

VIII.B Hard Information

Given the formula for soft information loss in Equation (A.8.4), we can write the expected utility for the specialty and the government, respectively, as

$$\begin{aligned} E[u_S] &= -E[(\theta + \theta_R - p)^2] - b^2 - c(L) \\ &= -\frac{1}{12} \left(\frac{L^2}{n^2} + A_n b^2 \right) - b^2 - c(L), \end{aligned} \quad (\text{A.8.5})$$

and as

$$\begin{aligned} E[u_G] &= -E[(\theta + \theta_R - p)^2] - b_R^2 \\ &= -\frac{1}{12} \left(\frac{L^2}{n^2} + A_n b^2 \right) - b_R^2. \end{aligned} \quad (\text{A.8.6})$$

In both Equations (A.8.5) and (A.8.6), n is the number of partitions supported by b and L and is given by Equation (A.8.1). Better information, either hard or soft, increases the utility of both the specialty and the government.

Taking the partial derivative of expected specialty utility with respect to L , while holding b and n fixed, yields the following condition for the agent's choice of L :

$$\frac{\partial}{\partial L} E[u_S] = -\frac{L}{6n^2} - c'(L) = 0. \quad (\text{A.8.7})$$

The convexity of $c(L)$ implies that there exists a single optimal candidate that satisfies Equation (A.8.7) for the cheap talk equilibrium with n partitions. Denote the solution to Equation (A.8.7) for a given n , if it exists (i.e., $n^*(b, L_n^*) = n$), as L_n^* .¹³ Intuitively, L_n^* is increasing in n : better soft communication

¹³In Equation (A.8.7), L_n^* is increasing in n , and in Equation (A.8.1), $n^*(b, L)$ is increasing in L . Since (i) $L_n^* \in (0, 1]$ and

(higher n) reduces the incentive to produce hard information (larger L_n^*). The globally optimal L^* is then given by $L^* = \arg \max_n (E[u_S; L_n^*])$. L^* is decreasing in b : As the specialty and the RUC have divergent preferences, soft communication worsens, and this increases the optimal hard information. Because the set of L_n^* comprises discrete values, $L^*(b)$ is a step function.

VIII.C Optimal RUC Bias

Because smaller L^* increases government utility in Equation (A.8.6), and because L^* is a decreasing function of $b = b_R - b_S$, the optimal b_R^* from the government's perspective is weakly lower under the possibility of hard information than when we fix $L = 1$.

However, the optimal $b_R^* \geq 0$. That is, an *adversarial* RUC is still never optimal from the government's perspective. In order for $b_R^* < 0$, we need three requirements:

1. The threshold \bar{b}_R where the specialty is indifferent between $n = 1$ and $n = 2$ must be less than 0.
2. The expected government utility when $b_R = \bar{b}_R$ is higher than the maximum expected government utility under $n = 2$:

$$\max E[u_G | n = 2] < E[u_G | b_R = \bar{b}_R].$$

3. The expected government utility when $b_R = \bar{b}_R$ is higher than complete delegation when $b_R = b_S$.

Note also that convexity of $c(L)$ implies that $c'(L_1^*) < c'(L_2^*)$. From the first order conditions that $c'(L_1^*) = -\frac{1}{6}L_1^*$ and $c'(L_2^*) = -\frac{1}{24}L_2^*$, we must have $L_1^* > \frac{1}{4}L_2^*$. Convexity also implies that

$$\frac{c(L_1^*) - c(L_2^*)}{L_2^* - L_1^*} \in \left[\frac{1}{24}L_2^*, \frac{1}{6}L_1^* \right].$$

The threshold \bar{b}_R is defined by the following condition:

$$E[u_G | b_R = \bar{b}_R, n = 1] = E[u_G | b_R = \bar{b}_R, n = 2].$$

In other words

$$\frac{1}{12}(L_1^*)^2 + (\bar{b}_R - b_S)^2 + c(L_1^*) = \frac{1}{48}(L_2^*)^2 + 2(\bar{b}_R - b_S)^2 + c(L_2^*).$$

The threshold is then

$$b_S = \bar{b}_R + \sqrt{\frac{1}{12}(L_1^*)^2 - \frac{1}{48}(L_2^*)^2 + c(L_1^*) - c(L_2^*)}. \quad (\text{A.8.8})$$

(ii) $n^*(b, L)$ is bounded by $n^*(b, 1)$, there must be at least one $n \in \{1, \dots, n^*(b, 1)\}$ such that $n^*(b, L_n^*) = n$.

Condition 1 and convexity imply that

$$b_S < \sqrt{\frac{1}{12} (L_1^*)^2 - \frac{1}{48} (L_2^*)^2 + \frac{1}{6} L_1^* (L_2^* - L_1^*)}. \quad (\text{A.8.9})$$

Condition 2 requires that

$$-\frac{1}{12} (L_1^*)^2 - \bar{b}_R^2 > -\frac{1}{48} (L_2^*)^2 - \frac{1}{2} b_S^2, \quad (\text{A.8.10})$$

where the expression on the left is the expected government utility at \bar{b}_R and $n = 1$, and the expression on the right is the expected government utility under the optimal $b_R = \frac{1}{2} b_S$ conditional on $n = 2$. Condition 3 requires that

$$-\frac{1}{12} (L_1^*)^2 - \bar{b}_R^2 > -b_S^2. \quad (\text{A.8.11})$$

The expression on the right is the government utility under full delegation.

We show numerically that there are no values $(L_1^*, L_2^*, b_S, \bar{b}_R)$ that satisfy Equations (A.8.8) to (A.8.11) simultaneously.

VIII.D Uniform Posterior Intervals

While it is convenient to work with continuous L , there is a technical complication in specifying values of $\underline{\theta}$ and $\bar{\theta}$, such that it remains that $\theta \sim U(\underline{\theta}, \bar{\theta})$ with fixed $L = \bar{\theta} - \underline{\theta}$. For example, consider the case of $L = 0.9$. If $\theta = 0$, then we must have $\underline{\theta} = 0$ with probability 1, but $\bar{\theta} = 0$ with probability less than 1 if $\theta > 0$. Therefore, if any potential interval must have $L = 0.9$, and we have a realized interval $[\underline{\theta}, \bar{\theta}] = [0, 0.9]$, then θ cannot be uniformly distributed within the realized interval.

To preserve uniform posterior distributions within the intervals revealed after hard information, we need sets of potential intervals to be mutually exclusive and collectively exhaustive. Thus, we may have one potential interval of length $L_a = 0.9$ and another potential interval of length $L_b = 0.1$. The ordering of these intervals may be random, but so long as the intervals are not overlapping in a particular ordering, then the posterior distribution of θ within each interval will remain uniform. We operationalize this with the concept that L instead represents the *expected* length of the information interval after hard information, under a mechanism that divides the unit interval into N intervals of length L_a and a remaining weakly shorter interval of length $L_b = 1 - NL_a \leq L_a$.

The probability that θ falls in an interval of length L_a is NL_a , while the probability that θ falls in the remaining interval of length L_b . Thus $L = NL_a^2 + L_b^2 = NL_a^2 + (1 - NL_a)^2$. We can solve for $L_a(L)$, as a function of L , by using the quadratic formula and the fact that $N = \lfloor L^{-1} \rfloor$:

$$L_a(L) = \frac{1 + \sqrt{1 - (1 - L) (\lfloor L^{-1} \rfloor^{-1} + 1)}}{1 + \lfloor L^{-1} \rfloor},$$

which is continuous and monotonically increasing in L .

We modify our equilibrium analysis by stating expected utility $E[u_A]$ (prior to hard information) as a function of L :

$$\begin{aligned} E[u_A] &= -E[(\theta - p)^2] - b^2 - c(L) \\ &= -\frac{1}{12} \left[\frac{NL_a^3}{n_a^2} + \frac{(1 - NL_a)^3}{n_b^2} + \bar{A}b^2 \right] - b^2 - c(L), \end{aligned} \quad (\text{A.8.12})$$

where $n_a = n^*(b, L_a)$, $n_b = n^*(b, 1 - NL_a) \leq n_a$, and $\bar{A} = NL_a A_{n_a} + (1 - NL_a) A_{n_b}$. The expression for the variance $E[(\theta - p)^2]$ is continuous, monotonically increasing in L (and $L_a(L)$), and piecewise convex in $L_a(L)$. The remainder of the analysis proceeds by identifying solutions $L_{\mathbf{n}}^*$, where $\mathbf{n} = (n_a, n_b)$, and choosing $L^* = \arg \max_{\mathbf{n}} (E[u_S; L_{\mathbf{n}}^*])$.

IX Private Price Transmission Robustness

In Section 5.3, we show that private insurance price changes are more responsive to Medicare price changes when the Medicare price changes originate from RUC decisions and, within RUC decisions, when they originate from a higher-affiliation proposal. We interpret this finding as supporting the hypothesis that RUC decisions, particular those from higher-affiliation proposals, contain valuable information that private insurance follows. In this appendix, we investigate alternative mechanisms that may generate this result.

First, affiliated proposals may result in more informative Medicare prices not because they facilitate communication, as detailed in Section 5, but because RUC members may naturally have more information about the procedures that their specialty societies perform. We investigate this possibility by using proxy measures of the RUC members' own information, based on their utilization of the service in question. In particular, we consider a specialty s 's share of total utilization for service i , w_{is} , as defined in Equation (5), and the service i 's share of the total utilization for specialty s , as defined in (2), averaging across the specialties of RUC members at the relevant meeting:

$$\bar{w}_{iy} = \frac{1}{\|\mathcal{R}_t(i, y)\|} \sum_{s \in \mathcal{R}_t(i, y)} w_{is}; \quad (\text{A.9.1})$$

$$\bar{\sigma}_{iy} = \frac{1}{\|\mathcal{R}_t(i, y)\|} \sum_{s \in \mathcal{R}_t(i, y)} \sigma_{is}, \quad (\text{A.9.2})$$

where $\mathcal{R}_t(i, y)$ is the set of RUC member specialties at the meeting $t(i, y)$ corresponding to service i and (private) price change year y .

Second, affiliated proposals may disproportionately represent high-volume services for which both private insurers and Medicare have interests in setting accurate prices. Strong correlation between private insurance and Medicare price changes for high-affiliation proposals may then result from careful

price-setting in both private insurance and Medicare, and not because affiliation *per se* causes better communication between proposing specialties and the RUC. We consider two measures of volume for service i : private insurance volume and total (private insurance and Medicare) volume.

Third, we take an omnibus approach, agnostic to the exact forces that may drive greater price following from Medicare to private insurance, by fitting a predictive model of price following. We consider changes in private insurance prices as a function of changes in Medicare prices:

$$\Delta \ln \text{Price}_{i,y}^P = \alpha + \beta_{iy} \Delta \ln \text{Price}_{i,y^M(i,y)}^M + \varepsilon_{iy},$$

where the goal is to predict β_{iy} .¹⁴ To operationalize this approach, as an approximation of β_{iy} , we take the ratio of demeaned $\Delta \ln \text{Price}_{i,y}^P$ and demeaned $\Delta \ln \text{Price}_{i,y^M(i,y)}^M$,

$$\text{Ratio}_{iy} = \frac{\overline{\Delta \ln \text{Price}_{i,y}^P} - \overline{\Delta \ln \text{Price}^P}}{\overline{\Delta \ln \text{Price}_{i,y^M(i,y)}^M} - \overline{\Delta \ln \text{Price}^M}},$$

where $\overline{\Delta \ln \text{Price}^P}$ and $\overline{\Delta \ln \text{Price}^M}$ are respective sample means of log private and Medicare price changes, weighted by Medicare volume. We then predict this ratio as a linear function of private insurance volume for i ; total (private insurance and Medicare) volume for i ; time dummies \mathbf{T}_{iy} for $y^M(i,y)$, y , and RUC meeting; and the vector of specialty shares \mathbf{w}_i . We take the predicted ratio, $\widehat{\text{Ratio}}_{iy}$, as an index for predicted price-following based on characteristics of (i,y) .

Given each of these measures that may influence price transmission to private insurance, we assess the robustness of our results to controlling for these measures, both directly and interacted with Medicare prices. Specifically, for each Index_{it} measure (i.e., \bar{w}_{iy} , $\bar{\sigma}_{iy}$, private volume of i , total volume of i , and $\widehat{\text{Ratio}}_{iy}$), we assess price transmission controlling for these proxy measures directly and interacted with Medicare prices, σ_{is} , in regressions similar to Equation (8):

$$\begin{aligned} \ln \text{Price}_{iy}^P &= \sum_c \left(\alpha_c + \beta_c \ln \text{Price}_{i,y^M(i,y)}^M \right) \cdot \mathbf{1}(c(i,y) = c) + \\ &\quad \sum_{\tau=1}^3 \left(\gamma_\tau + \delta_\tau \ln \text{Price}_{i,y^M(i,y)}^M \right) \cdot \mathbf{1} \left(F(\text{Index}_{iy}) \in \left(\frac{\tau-1}{3}, \frac{\tau}{3} \right) \right) + \\ &\quad \mathbf{T}_{iy} \eta + \xi_i + \varepsilon_{iy}, \end{aligned} \tag{A.9.3}$$

where $\tau \in \{1,2,3\}$ indicates the tercile, $F(\cdot)$ is the distribution function of the relevant measure Index_{it} , and the rest is the same as in Equation (8). Appendix Table A.9 shows results from these regressions. The key coefficients of interest, β_C , are highly stable regardless of Index_{iy} . Price transmission remains greater for Medicare price changes originating from RUC decisions and, within these decisions, from high-affiliation proposals.

¹⁴This changes-on-changes specification closely matches the fixed-effects specification in Equation (8). As shown in Appendix Figure A.14, separating Medicare price changes into high- and low-affiliation groups gives similar results.

Table A.1: Sample Selection

Sample step	Description	Observations	
		Dropped	Remaining
1. Raw RUC data	Universe of all administrative data used by RUC		17,498
2. Drop observations with no survey information and no RUC recommendation	These observations do not represent RUC decisions, as all decisions require these elements	11,079	6,419
3. Drop observations that appear to be duplicates	Identify observations with the same CPT code, RUC meeting, and survey specialty; if there are differences in other variables between these observations, choose the observation with the most complete data and larger survey sample sizes	132	6,353
4. Combine observations with same CPT code and RUC meeting but different survey specialties	These observations were incorrectly entered as separate lines; use total survey sample and respondent numbers	127	6,226
5. Drop observations with invalid RUC meeting date	83% of these observations have a meeting date of “Editorial,” indicating that the RUC decided that a full decision was not necessary, and no specialty proposals were elicited; 10% of these observations are “HCPAC,” which are not for physician procedures	490	5,736
6. Drop observations with missing survey specialty or specialties	These observations are likely administrative discussions without a full proposal from a specialty or specialties	1,313	4,423
7. Drop observations involving proposing specialties with missing affiliation measures	These involve rare specialty societies that cannot be identified in the Medicare or MarketScan claims	16	4,407

Notes: This table describes key sample selection steps, the observations dropped, and the observations remaining after each step. The sample selection steps were taken after detailed discussions with the RUC to understand their data and aim to retain observations that represent full RUC decisions with a specialty proposal.

Table A.2: Example CPT Descriptions

CPT code	Short description	Long description
99214	Office / outpatient visit, established	Office or other outpatient visit for the evaluation and management of an established patient, which requires at least 2 of these 3 key components: A detailed history; A detailed examination; Medical decision making of moderate complexity. Counseling and/or coordination of care with other physicians, other qualified health care professionals, or agencies are provided consistent with the nature of the problem(s) and the patient's and/or family's needs. Usually, the presenting problem(s) are of moderate to high severity. Typically, 25 minutes are spent face-to-face with the patient and/or family.
71010	Chest x-ray 1 view frontal	Radiologic examination, chest; single view, frontal
17003	Destruct premalignant lesion 2-14	Destruction (e.g., laser surgery, electrocautery, cryosurgery, chemosurgery, surgical curettement), premalignant lesions (e.g., actinic keratoses); second through 14 lesions, each (List separately in addition to code for first lesion)
95165	Antigen therapy services	Professional services for the supervision of preparation and provision of antigens for allergen immunotherapy; single or multiple antigens (specify number of doses)
44391	Colonoscopy for bleeding	Colonoscopy through stoma; with control of bleeding (e.g., injection, bipolar cautery, unipolar cautery, laser, heater probe, stapler, plasma coagulator)
96413	Chemo iv infusion 1 hr	Chemotherapy administration, intravenous infusion technique; up to 1 hour, single or initial substance/drug
20610	Drain/inject joint/bursa	Arthrocentesis, aspiration and/or injection; major joint or bursa (e.g., shoulder, hip, knee joint, subacromial bursa)
62311	Inject spine lumbar/sacral	Injection(s), of diagnostic or therapeutic substance(s) (including anesthetic, antispasmodic, opioid, steroid, other solution), not including neurolytic substances, including needle or catheter placement, includes contrast for localization when performed, epidural or subarachnoid; lumbar or sacral (caudal)

Notes: This table shows short and long descriptions of example CPT codes, determined by the AMA CPT Committee prior to a proposal to the RUC. Stem words in the long description are used for predicting RVUs after LASSO selection.

Table A.3: Price Effect of Alternative Affiliation Measures

<i>Data</i>	(1)	(2)	(3)	(4)	(5)
	<i>Affiliation metric</i>				
	Euclidean	Gini-Euclidean	Manhattan	σ -Cosine	w -Cosine
Panel A: Mean affiliation					
Medicare CPT quantity	0.101*** (0.029)	0.103*** (0.030)	0.055** (0.021)	0.061** (0.025)	0.033** (0.015)
Medicare + MarketScan CPT quantity	0.076*** (0.025)	0.079*** (0.026)	0.048** (0.020)	0.057** (0.025)	0.028* (0.015)
Medicare CPT revenue	0.094*** (0.029)	0.094*** (0.029)	0.038* (0.019)	0.037* (0.021)	0.033** (0.015)
Medicare BETOS quantity	0.088*** (0.029)	0.088*** (0.030)	0.056** (0.022)	0.052** (0.025)	0.036** (0.016)
Medicare BETOS revenue	0.072*** (0.027)	0.069** (0.028)	0.045** (0.021)	0.032 (0.020)	0.036** (0.015)
Panel B: 33rd percentile affiliation					
Medicare CPT quantity	0.104*** (0.032)	0.111*** (0.031)	0.061** (0.024)	0.060** (0.026)	0.026* (0.014)
Medicare + MarketScan CPT quantity	0.076*** (0.024)	0.082*** (0.026)	0.062** (0.023)	0.051** (0.024)	0.027* (0.013)
Medicare CPT revenue	0.089*** (0.031)	0.092*** (0.033)	0.039* (0.021)	0.027 (0.022)	0.027* (0.014)
Medicare BETOS quantity	0.086** (0.033)	0.093*** (0.034)	0.066*** (0.025)	0.054** (0.026)	0.038** (0.018)
Medicare BETOS revenue	0.088*** (0.029)	0.085*** (0.029)	0.053** (0.022)	0.043** (0.018)	0.034** (0.016)

Notes: This table shows results of regressions of log RVU on various measures of set affiliation. Each cell represents the coefficient on the affiliation measure in a separate regression, stated as α in Equation (6) and corresponding to the preferred specification of column (4) in Table III. Further details about the regression controls are given in the note for Table III. Rows of the table correspond to underlying data from which affiliation is calculated. Columns correspond to affiliation metrics between two specialties, discussed in Appendix II. Appendix II.A discusses the baseline metric of Euclidean distance, shown in column (1), in detail, including differences in interpreting using quantity vs. revenue shares. The remaining affiliation metrics are described in Appendix II.B. Panel A calculates the set affiliation measure as the mean maximized specialty-pair affiliation, which is the default and is given in Equation (4). Panel B calculates the set affiliation measure as the 33rd percentile of the maximized specialty-pair affiliations. Standard errors, clustered by RUC meeting, are in parentheses; *** denotes significance at the 1% level.

Table A.4: Alternative Mechanisms Behind Price Effect

	(1)	(2)	(3)	(4)	(5)
	Log RVU				
Standardized set affiliation	0.098*** (0.029)	0.103*** (0.030)	0.104*** (0.029)	0.098*** (0.029)	0.112*** (0.043)
Standardized measures of RUC-specialty interest					
Mean σ_{is}^q	0.021** (0.009)				
Mean σ_{is}^R		0.031*** (0.007)			
Mean $\tilde{\sigma}_{is}^q$			0.052** (0.012)		
Mean $\tilde{\sigma}_{is}^R$				0.048*** (0.013)	
Baseline controls	Y	Y	Y	Y	Y
Proposer count dummies	N	N	N	N	Y
N	4,401	4,401	4,401	4,401	4,401
Adjusted R -squared	0.891	0.895	0.892	0.892	0.891
Sample mean log RVU	1.567	1.567	1.567	1.567	1.567

Notes: This table shows results of regressions of log RVU on standardized set affiliation, with the addition of controls to test robustness to alternative mechanisms. Columns (1) to (4) relate to alternative mechanisms of service-specific interests or *ex ante* information held by RUC specialties. These specifications, given in Equation (A.6.1), control for mean direct interests (σ_{is}^q and σ_{is}^R in columns (1) and (2), respectively) or related interests ($\tilde{\sigma}_{is}^q$ and $\tilde{\sigma}_{is}^R$ in columns (3) and (4), respectively) across RUC specialties. Measures are standardized to have mean 0 and standard deviation 1. Column (5) tests robustness to the alternative mechanism of signaling “buy-in,” controlling for proposer dummies, as in Equation (A.6.2). Details are given in Appendix VI. All specifications include controls in the baseline price-effect regression, in column (4) of Table III. Standard errors, clustered by RUC meeting, are in parentheses; ** denotes significance at the 5% level, and *** denotes significance at the 1% level.

Table A.5: Tabulation of Proposal Types

Prior existence	Quantity		Total
	Low	High	
Existing	967	1,394	2,361
New	1,167	740	1,907
Total	2,134	2,134	4,268

Prior existence	Price		Total
	Low	High	
Existing	180	2,201	2,381
New	2,026	0	2,026
Total	2,206	2,201	4,407

Quantity	Price		Total
	Low	High	
Low	1,179	955	2,134
High	908	1,226	2,134
Total	2,087	2,181	4,268

Notes: This table shows counts of proposals along three binary dimensions: (i) CPT code is existing or new at the time of the proposal, (ii) CPT code has an RVU that is below- or above-median, and (iii) CPT code has yearly frequencies in the Medicare data that is below- or above-median, for years that the CPT code was in existence.

Table A.6: Heterogeneous Effect of Affiliation by Proposal Type

	(1)	(2)	(3)	(4)
	Log RVU			
Standardized set affiliation				
× existing CPT	-0.035 (0.031)			
× new CPT	0.209*** (0.030)			
× low-quantity CPT		0.169*** (0.033)		
× high-quantity CPT		0.034 (0.034)		
× low-priced CPT			0.160*** (0.027)	
× high-priced CPT			-0.034 (0.028)	
× early meeting				0.097* (0.049)
× late meeting				0.104*** (0.036)
Baseline controls	Y	Y	Y	Y
<i>N</i>	4,401	4,262	4,401	4,401
Adjusted <i>R</i> -squared	0.896	0.895	0.894	0.891
Sample mean outcome	1.567	1.595	1.567	1.567

Notes: This table shows results of regressions of log RVU on standardized set affiliation interacted with indicators of a proposal type, as stated in Equation (A.7.1). Four types of binary proposal heterogeneity are considered: (i) whether the proposal is for an existing CPT code, in column (1), (ii) whether the proposal is for a CPT code with below- or above-median quantity per year (in years the CPT was in existence), in column (2), (iii) whether the proposal is for a CPT code with below- or above-median price, in column (3), and (iv) whether the proposal occurred in an earlier (before the third meeting in 2005) or later (at or after the third meeting in 2005) RUC meeting, column (4). Tabulations of proposals across the first three characteristics are given in Appendix Table A.5. Baseline controls are the same as in column (5) of Table III. Standard errors, clustered by RUC meeting, are in parentheses; ** denotes significance at the 5% level, and *** denotes significance at the 1% level.

Table A.7: Specialty Seats on Counterfactual RUC

Specialty	Seats	Specialty	Seats
Anesthesiology	2	Obstetrics and Gynecology	2
Cardiology	1	Oncology	1
Emergency Medicine	2	Ophthalmology	1
Family Medicine	4	Orthopedic Surgery	1
Gastroenterology	1	Pediatrics	2
General Surgery	1	Psychiatry	1
Internal Medicine	4	Radiology	1
Neurology	1		

Notes: This table shows members of a counterfactual RUC, in which seats are assigned in proportion to the population of physicians in each specialty. The number of total seats is 25, as it is in the current RUC. This RUC accommodates the 16 largest specialties; including specialties with fewer physicians would require a larger RUC. Many smaller specialties lack a seat in this RUC; compare this to the broader range of specialties that have some representation on the actual RUC over time in Table I. Physician population numbers are from Table 1.1 of Association of American Medical Colleges (2016), accessible at <https://www.aamc.org/data/workforce/reports/458480/1-1-chart.html>.

Table A.8: Affiliation Effect on Hard Information

	(1)	(2)	(3)
Panel A: Log survey sample			
Standardized set affiliation	-0.228*** (0.071)	-0.332*** (0.076)	-0.146** (0.070)
Baseline controls	Y	Y	Y
Utilization among proposers	N	Y	Y
Proposer count dummies	N	N	Y
<i>N</i>	4,407	4,219	4,219
Adjusted <i>R</i> -squared	0.329	0.332	0.348
Sample mean outcome	4.660	4.619	4.619
Panel B: Log survey respondents			
Standardized set affiliation	-0.219*** (0.076)	-0.413*** (0.049)	-0.082 (0.055)
Baseline controls	Y	Y	Y
Utilization among proposers	N	Y	Y
Proposer count dummies	N	N	Y
<i>N</i>	4,407	4,219	4,219
Adjusted <i>R</i> -squared	0.220	0.253	0.304
Sample mean outcome	3.067	3.071	3.071

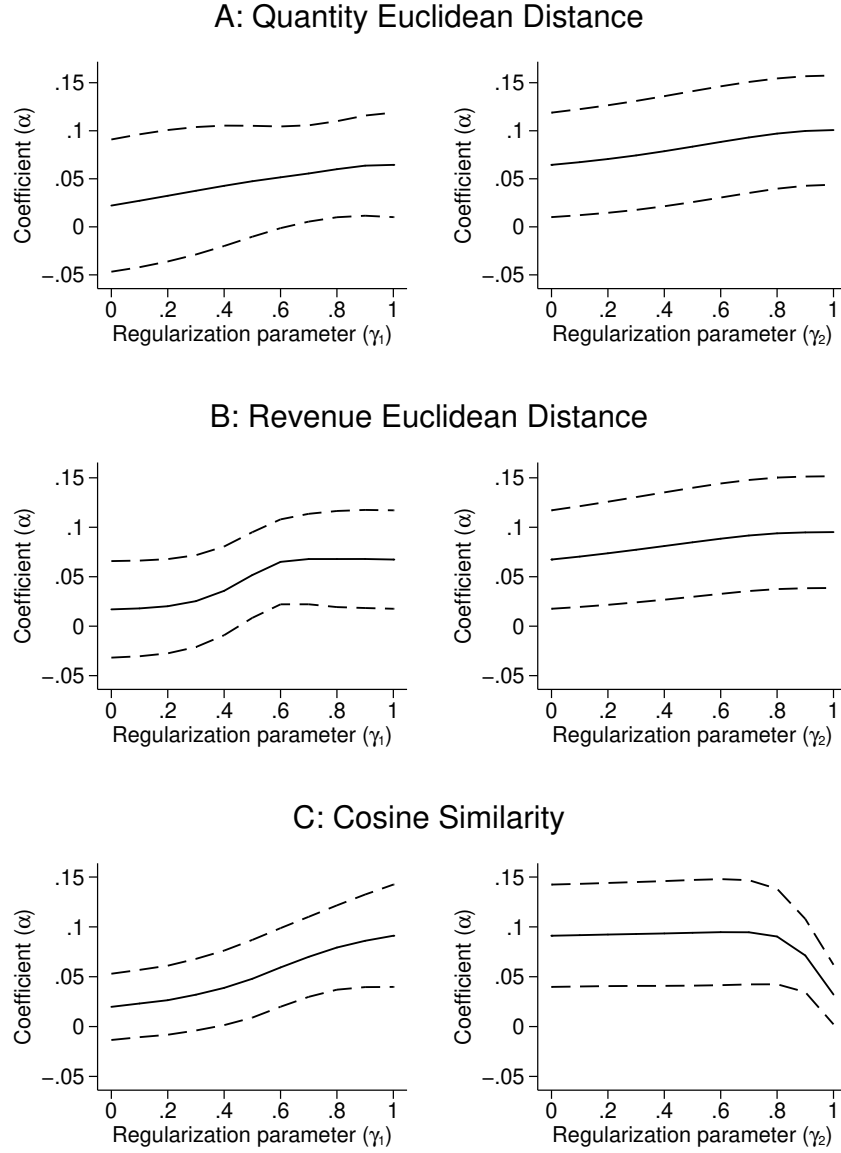
Notes: This table shows results of regressions of survey measures of hard information on standardized set affiliation, based on Equation (7). Survey sample regressions are shown in Panel A, and survey respondent regressions are shown in Panel B. The outcomes are per-specialty measures, constructed by dividing the total survey measures by the number of proposing specialties. Baseline controls are the same as in column (5) of Table III. Columns (2) and (3) control for the log annual utilization of the service among all specialties and the log annual utilization of the service among proposing specialties, dropping observations for which these values are missing. Column (3) also includes dummies for the proposing specialty count. Standard errors, clustered by RUC meeting, are in parentheses; ** denotes significance at the 5% level, and *** denotes significance at the 1% level.

Table A.9: Price Transmission Robustness

	(1)	(2)	(3)	(4)	(5)	(6)
	Log private price					
Log Medicare price						
× not RUC	0.331*** (0.022)	0.291*** (0.022)	0.328*** (0.022)	0.338*** (0.023)	0.329*** (0.022)	0.326*** (0.022)
× RUC, low affiliation	0.520*** (0.023)	0.513*** (0.027)	0.530*** (0.023)	0.536*** (0.024)	0.524*** (0.023)	0.520*** (0.023)
× RUC, high affiliation	0.642*** (0.041)	0.733*** (0.044)	0.653*** (0.041)	0.657*** (0.042)	0.655*** (0.041)	0.629*** (0.04)
RUC, high vs. low affiliation	-0.016 (0.067)	0.168** (0.069)	-0.017 (0.067)	-0.003 (0.067)	0.001 (0.068)	-0.048 (0.066)
Proxy or predictor ($\text{Index}_{i,y}$)	None	$\bar{w}_{i,y}$	$\bar{\sigma}_{i,y}$	Private volume	Total volume	All
N	7,182	7,182	7,182	7,182	7,182	7,182
Adjusted R -squared	0.852	0.859	0.852	0.987	0.987	0.987

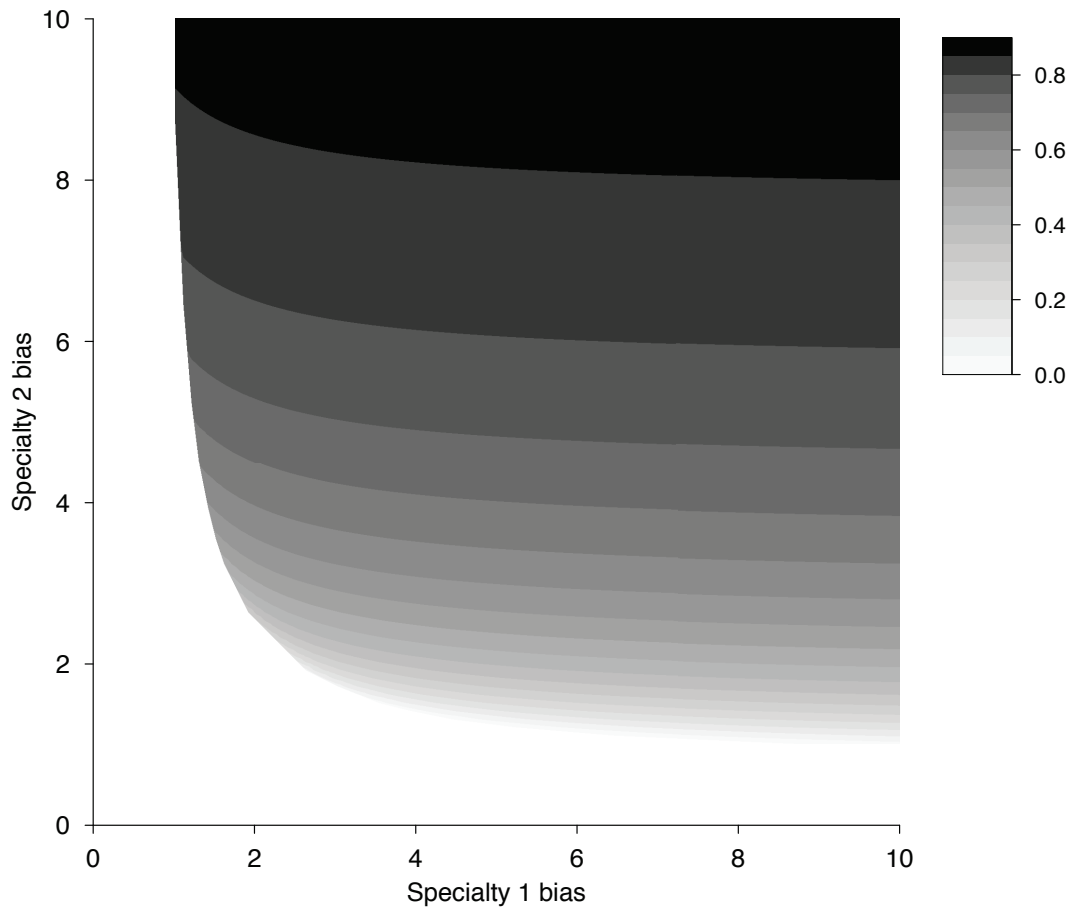
Notes: This table shows results of regressions of log private price on log Medicare price, as in Table IV. Definitions of private and Medicare prices and the merging of the two prices are given in Table IV. Column (1) has no proxy or predictor and is identical to column (5) in Table IV, as written in Equation (9). The remaining columns control for indicators of terciles of a proxy and interactions of these indicators with log Medicare price, as written in Equation (A.9.3). Columns (2) and (3) consider proxies for information that the average RUC member specialty may have about i , specifically $\bar{w}_{i,t}$ and $\bar{\sigma}_{i,t}$, defined as the average specialty share of a service's utilization and the average service share of a specialty's utilization, given in Equations (A.9.1) and (A.9.2), respectively. Columns (4) and (5) consider proxies of the importance of a service i to private insurance, specifically the private insurance volume or the total private insurance and Medicare volume, respectively. Column (6) considers an prediction of price transmission based on private volume, total volume, year dummies, Medicare price change year dummies, RUC meeting dummies, and specialty share w_i . All regressions are run on the same sample of 7,182 observations, weighted by Medicare volume. Standard errors are in parentheses. ** denotes significance at the 5% level; *** denotes significance at the 1% level.

Figure A.1: Regularized Affiliation Measures



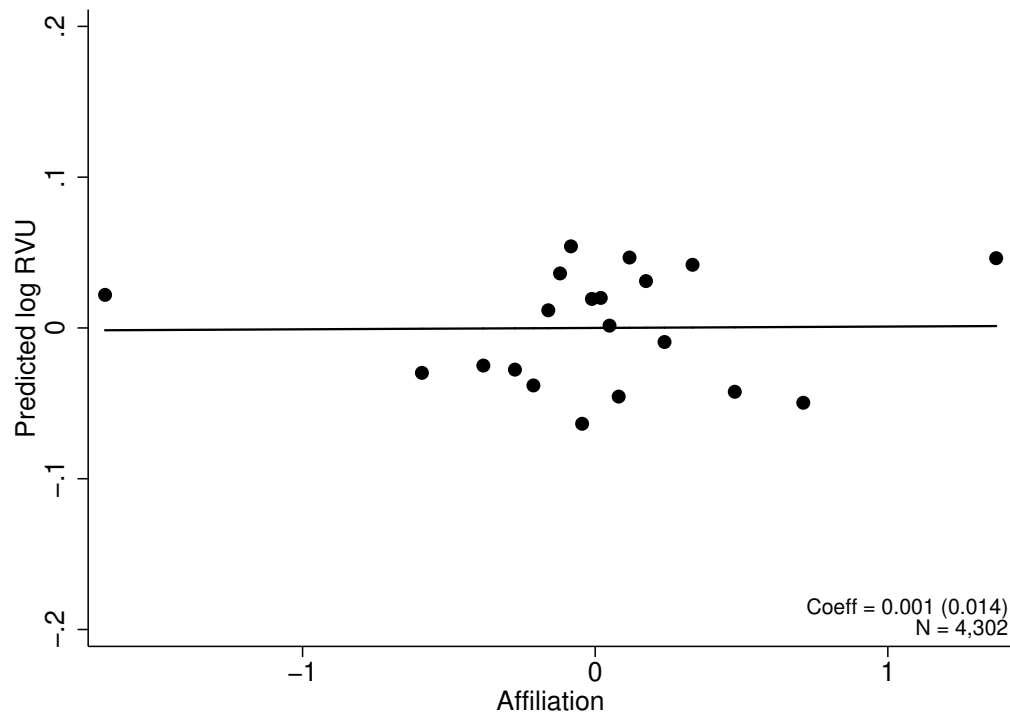
Notes: Each panel in this figure plots the effect of set affiliation based on regularized spillovers matrices: Euclidean distance in σ^q (Panel A), Euclidean distance in σ^R (Panel B), and w -cosine similarity (Panel C). The y-axis shows coefficient α from Equation (6) (baseline specification of column (4) in Table III) on the y-axis and a regularization parameter on the x-axis. Confidence intervals are shown as dashed lines. The left side of each panel varies a regularization parameter (γ_1) that varies $\Omega_{\gamma_1,0}$ from a variance-covariance matrix ($\gamma_1 = 0$) to a correlation matrix ($\gamma_1 = 1$). The right side of each panel varies a regularization parameter (γ_2) that transforms Ω_{1,γ_2} from a correlation matrix ($\gamma_2 = 0$) to an identity matrix ($\gamma_2 = 1$). Results on the left side of each panel hold fixed $\gamma_2 = 0$, and results on the right side hold fixed $\gamma_1 = 1$. The right-most result ($\gamma_2 = 1$) matches results in Appendix Table A.3, which are implicitly based on $\Omega_{1,1} = \mathbf{I}_C$. Details are discussed in Appendix II.C.

Figure A.2: Mixed Strategy Proposal Probabilities



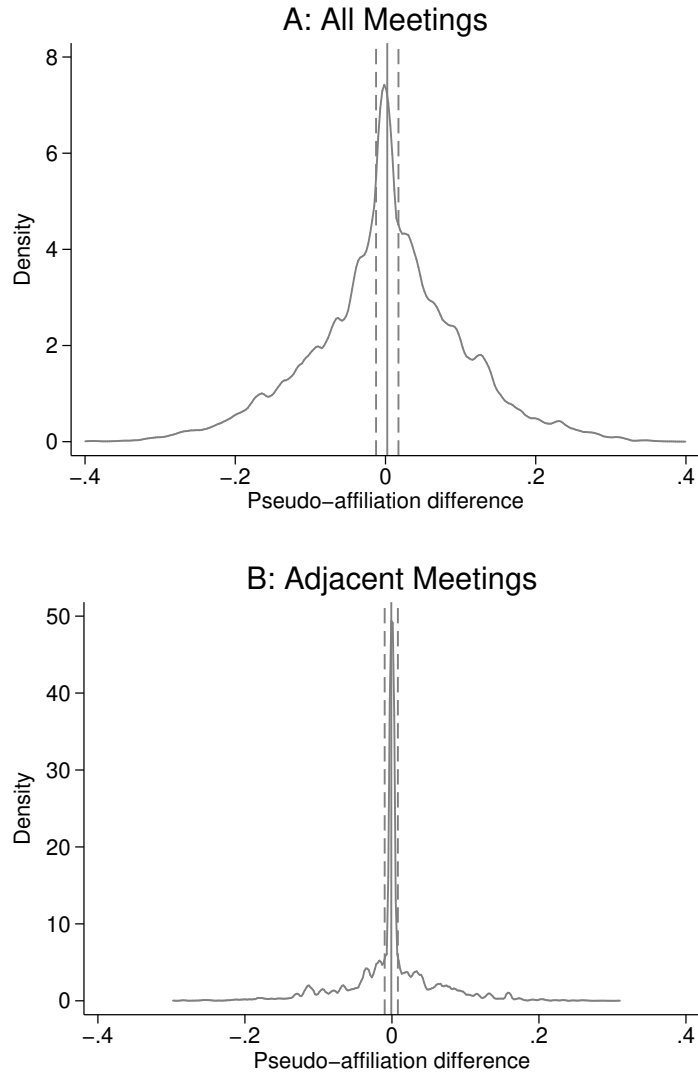
Notes: This figure shows the probability of proposal participation under $\theta = 1$ by specialty 1 in a mixed strategy equilibrium, in which specialties do not propose if $\theta = 0$ and mix if $\theta = 1$, described in Appendix III. Proposal probabilities are depicted in the space of bias by specialties 1 and 2. No mixed strategy equilibria exist in the region shown in pure white.

Figure A.3: Balance of Medicare Beneficiary Characteristics across Affiliation



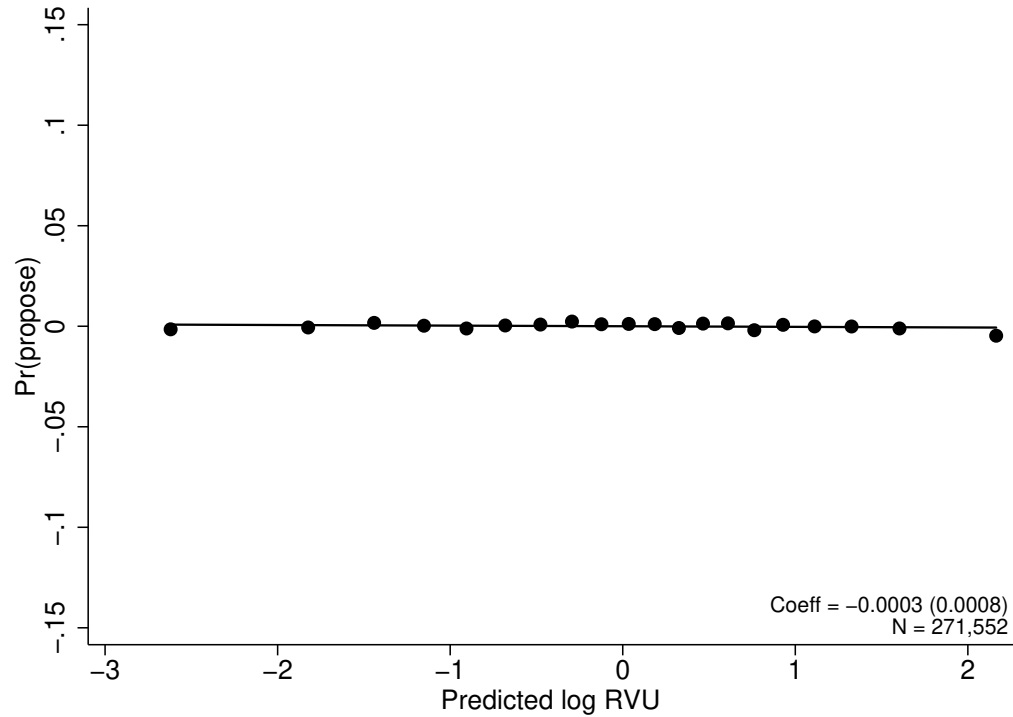
Notes: This figure is a binned scatterplot of residual predicted log RVU, based on Medicare beneficiary characteristics, on residual affiliation, where each dot represents 5% of the data, ordered by residual affiliations. Log RVU is first predicted by Medicare beneficiary characteristics, which are listed in Table II. The R -squared of this prediction equation is 0.249. Residuals are formed by regressing predicted log RVU and affiliation, respectively, on meeting dummies and specialty shares w_i . The line shows the best fit through the residualized data, with corresponding coefficient and standard error clustered by meeting.

Figure A.4: Random Timing of Proposals



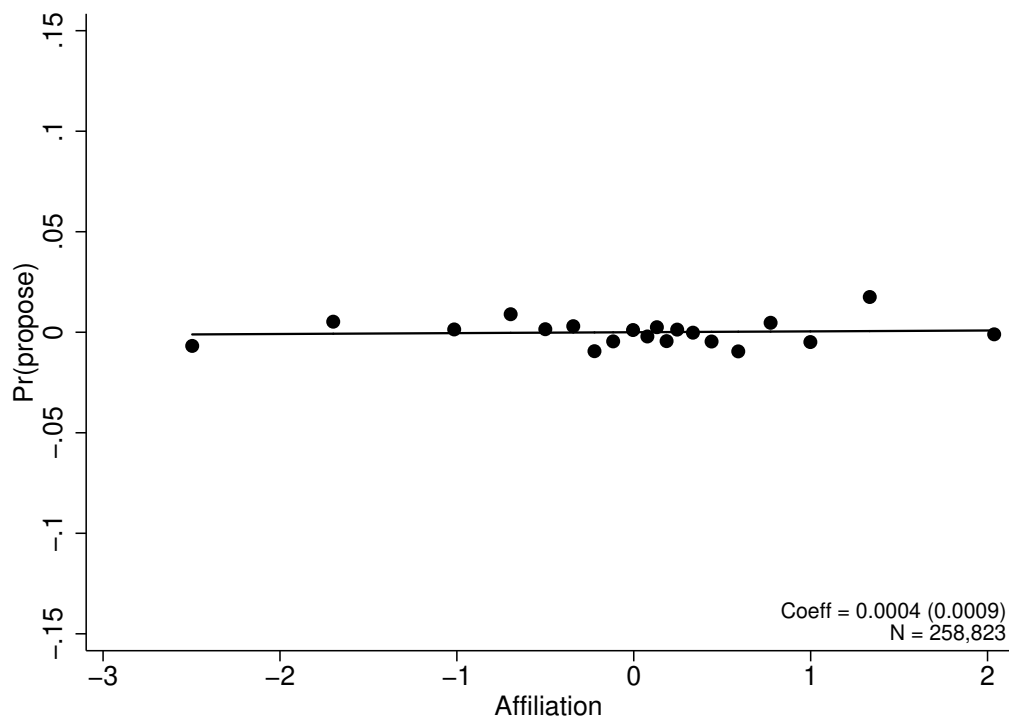
Notes: This figure shows the distribution of the difference between set affiliation in pseudo-meetings and the actual set affiliation of each proposal. All affiliation measures are standardized so that the distribution of actual set affiliation has a standard deviation of 1. In Panel A, we include all 60 meetings for every proposal. In Panel B, we include only meetings that were within three meetings (both earlier or later) of the actual meeting. The mean difference is shown as a solid vertical line. The 95% confidence interval, shown in dashed vertical lines, is calculated by a regression of the difference on a constant, clustering standard errors for meeting identifiers.

Figure A.5: Balance of Proposal Probability on Predicted Price



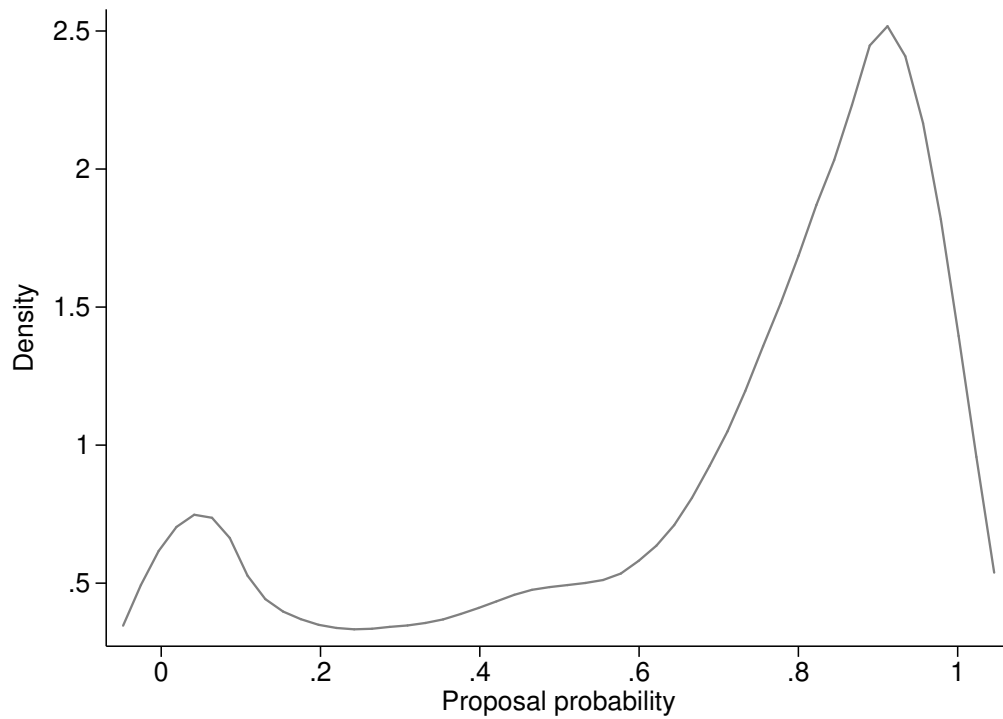
Notes: This figure is a binned scatterplot of residual proposal probability on residual predicted log RVU, where each dot represents 5% of the data, ordered by residual predicted log RVU. Each observation is a proposal-specialty pair, and the outcome variable of interest is an indicator for whether the specialty was part of that proposal. Log RVU is predicted from service (CPT code) characteristics, word descriptions, and prior RVU, which are described in Table III; the prediction equation has an adjusted R -squared of 0.88. The specialty proposal indicator and predicted log RVU are both residualized by the following predictors of proposing: specialty dummies for s , meeting dummies for t , Medicare utilization shares $w_{i,s}$ for specialty s out of total utilization for service i , and an indicator for whether $w_{i,s} = 0$. The standard deviation of the proposal propensities, detailed in Appendix IV, is 0.13 across proposal-specialty pairs, so that the span of the y -axis is approximately 1 standard deviation above and below. The line shows the best fit through the residualized data, with corresponding coefficient and standard error clustered by meeting.

Figure A.6: Random Proposals with Respect to Affiliation



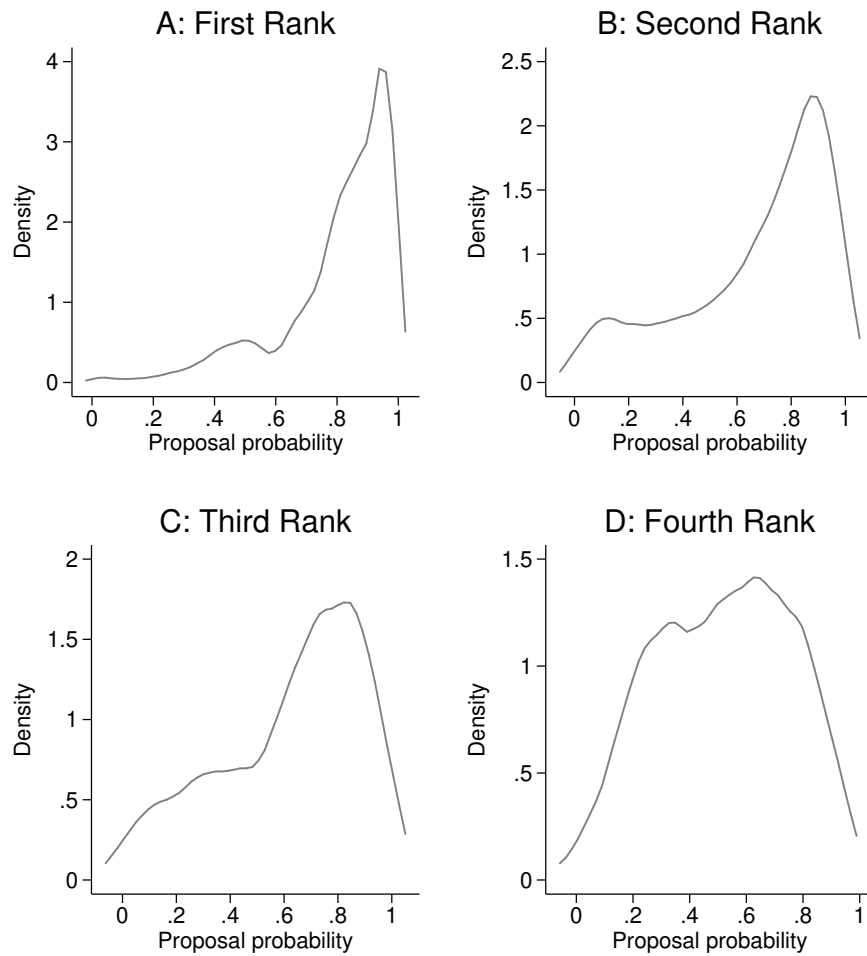
Notes: This figure is a binned scatterplot of residual proposal probability on affiliation between a specialty and the RUC, where each dot represents 5% of the data, ordered by residual affiliation. Each observation is a proposal-specialty pair, and the outcome variable of interest is an indicator for whether the specialty was part of that proposal. Affiliation is calculated between each potential proposing specialty s and the set of RUC specialties \mathcal{R}_t at the relevant meeting t , or $A(\mathcal{R}_t, s)$. The mean affiliation for specialty s across all meetings, or $\bar{A}(s) \equiv \|T\|^{-1} \sum_{t \in T} A(\mathcal{R}_t, s)$, is subtracted from this affiliation, and this difference $A(\mathcal{R}_t, s) - \bar{A}(s)$ is standardized to have mean 0 and standard deviation 1. The proposal-specialty indicator and affiliation are both residualized by indicators for the number of specialties on a given proposal and for the specialty identity. The standard deviation of the proposal propensities, detailed in Appendix IV, is 0.13 across proposal-specialty pairs, so that the span of the y-axis is approximately 1 standard deviation above and below. The line shows the best fit through the residualized data, with corresponding coefficient and standard error clustered by meeting.

Figure A.7: Distribution of Specialty-Proposal Propensities among Proposers



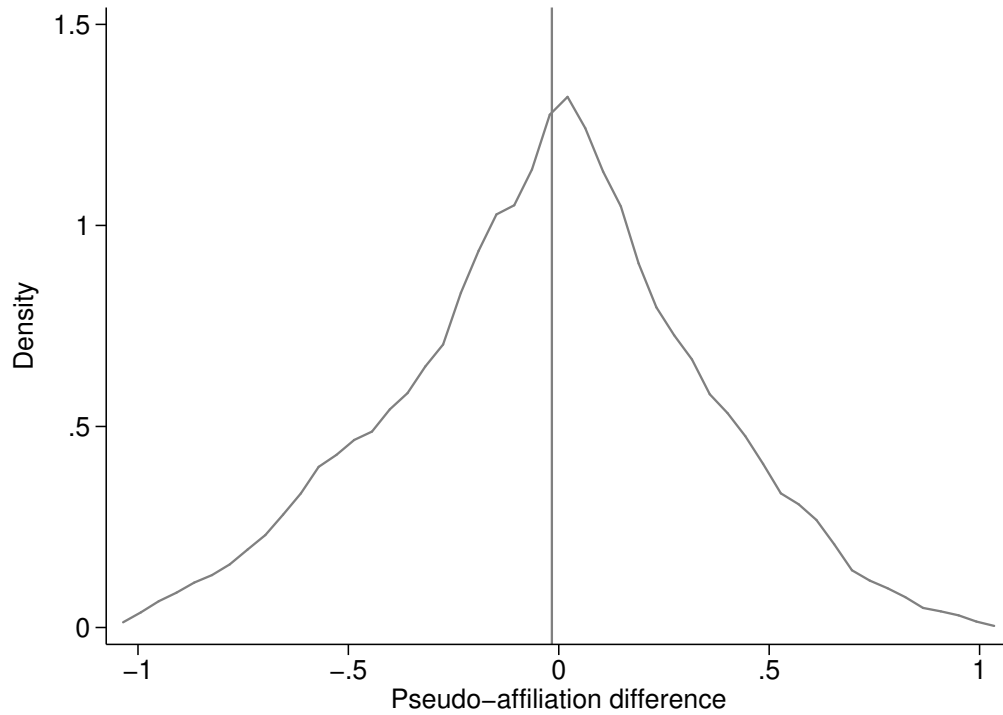
Notes: This figure shows the density of specialty-proposal propensities, estimated by a logit model of 248,735 specialty-proposal pairs as described in Appendix IV. Proposal propensities are shown for 6,929 actual specialty-proposal pairs over 4,199 proposals.

Figure A.8: Distribution of Highly Ranked Specialty-Proposal Propensities



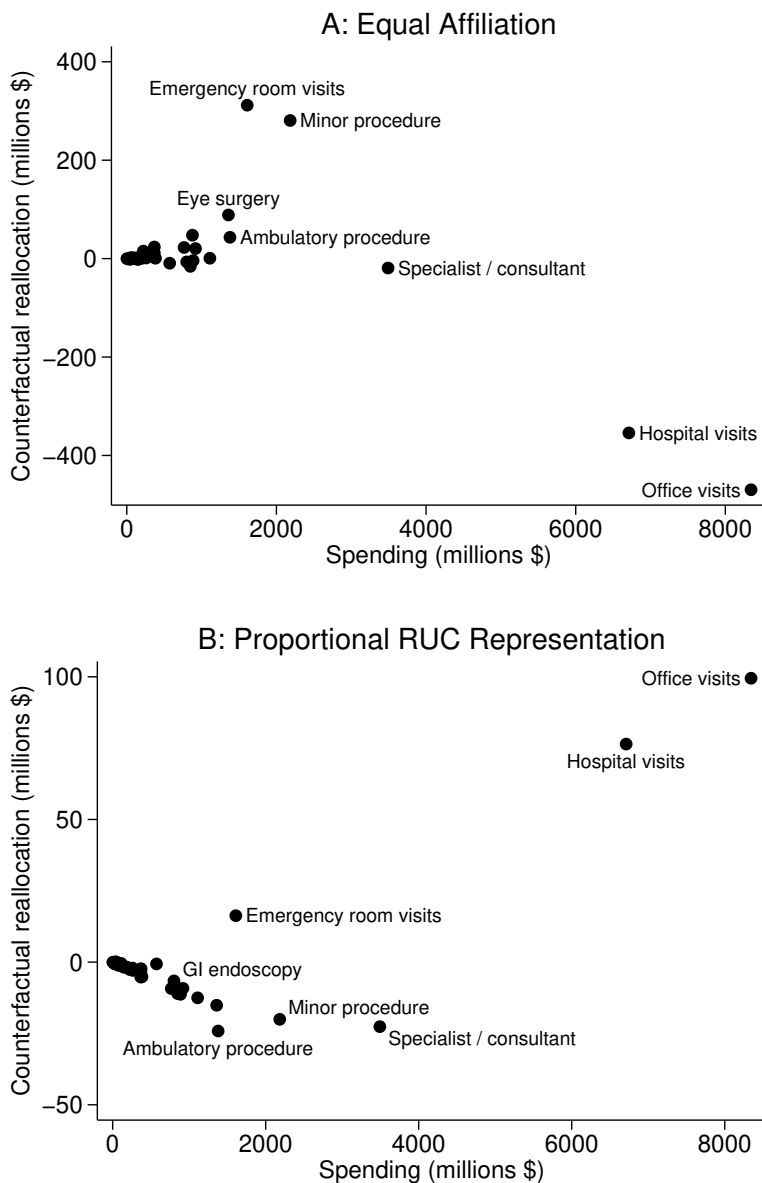
Notes: This figure shows the density of specialty-proposal propensities, estimated by a logit model of 248,735 specialty-proposal pairs as described in Appendix IV. In each panel, proposal propensities are shown only for correspondingly ranked specialty for proposals that have at least as many actual proposers. Specifically, in Panel A, the highest specialty propensity is shown for 4,199 proposals. In Panel B, the second-highest specialty propensity is shown for 1,524 proposals with at least two proposers. In Panel C, the third-highest specialty propensity is shown for 558 proposals with at least three proposers. In Panel D, the fourth-highest specialty propensity is shown for 300 proposals with at least four proposers.

Figure A.9: Distribution of Simulated Set Affiliation Relative to Actual Set Affiliation



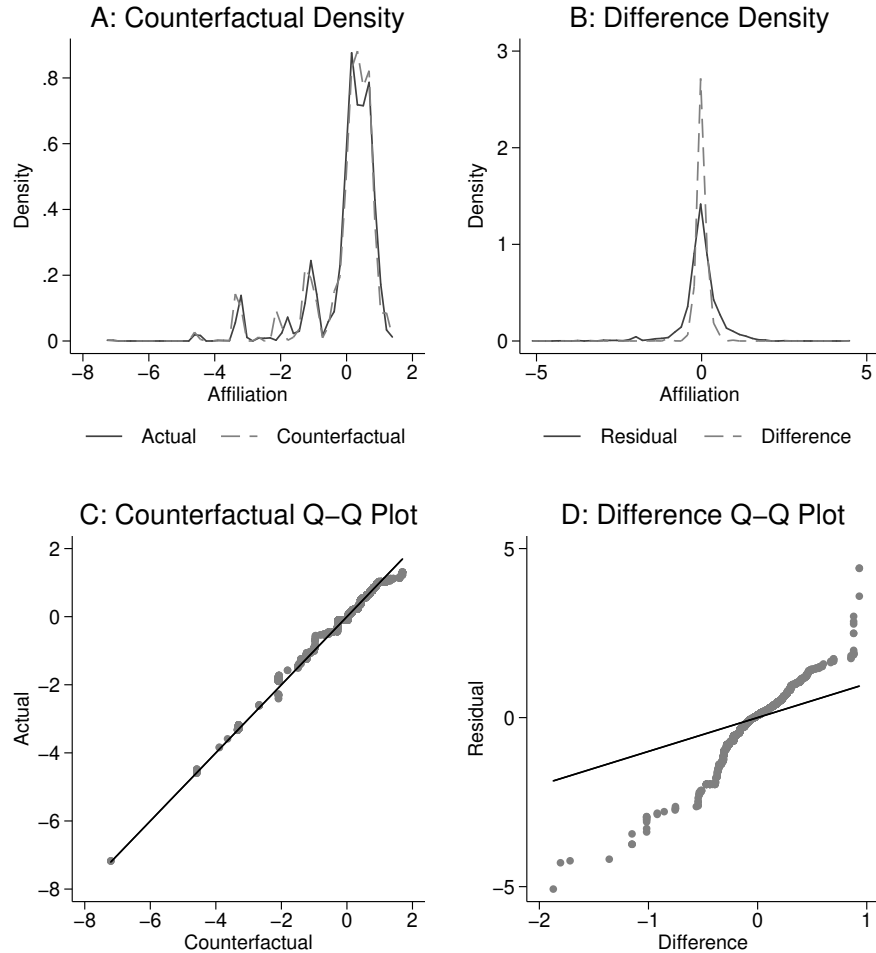
Notes: This figure shows the density of 51,763 simulated set affiliations, using actual \mathcal{R}_i and simulated proposing specialty sets \mathcal{S}_i for each proposal i , differenced by actual set affiliation. Simulated specialty-proposals are derived from a logit model of specialty-proposal propensities, as illustrated in Appendix Figures A.7 and A.8. Simulated observations are weighted by their likelihood of being drawn. The weighted standard deviation of the simulated set affiliations is 0.242, and the weighted mean of the differenced statistic is -0.016 . Details of the simulation algorithm are described in Appendix IV.

Figure A.10: Revenue Reallocation across Service Categories



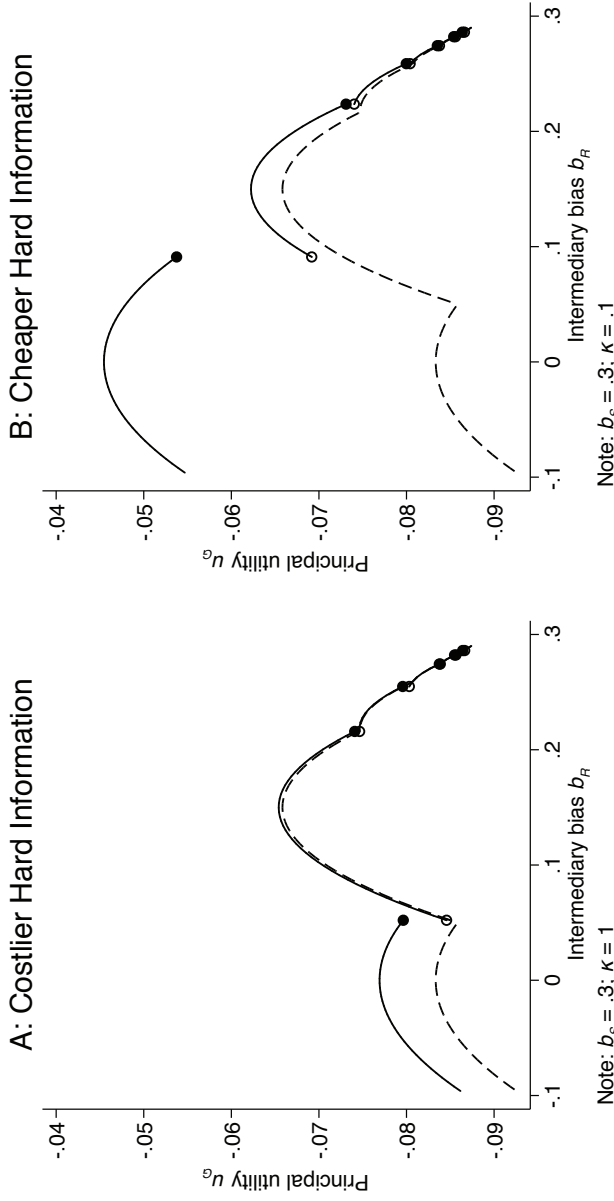
Notes: This figure shows counterfactual yearly revenue reallocation across Berenson–Eggers Type of Service (BETOS) service categories in two counterfactual scenarios. In Panel A, we consider equalizing the affiliation of all proposals in each year. In Panel B, we consider changing the RUC membership to be constant and proportional to the population of physician specialties in the US, as given in Appendix Table A.7. Average annual spending for each specialty is on the x -axis, while the counterfactual reallocation setting affiliation to the mean for all proposals is on the y -axis. Utilization quantities for each service (CPT code) is held fixed, and the annual Medicare budget for physician work is set at \$70 billion \times 51% = \$35.7 billion. Details are given in Section 4.2.

Figure A.11: Counterfactual and Actual Distributions of Affiliation



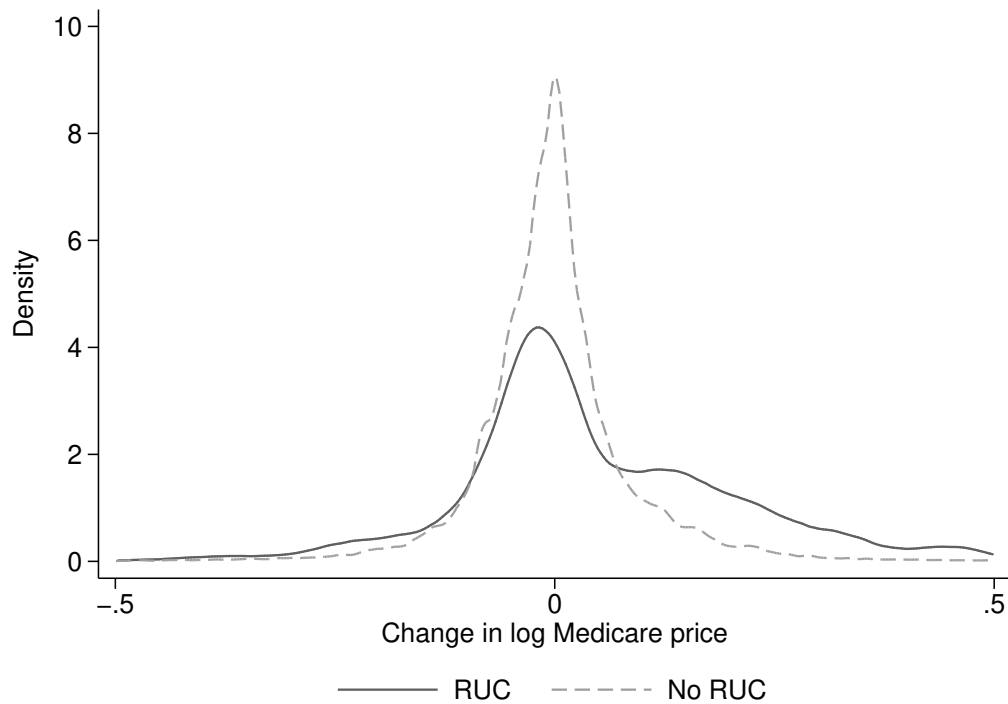
Notes: This figure compares counterfactual and actual distributions of affiliation. Affiliation is detailed in Section 3.3 and is a function of the set of proposing specialties \mathcal{S}_i for a proposal i and the set of RUC specialties \mathcal{R}_t during meeting t , or $A(\mathcal{R}_t, \mathcal{S}_i)$. The counterfactual affiliation for proposal i is given by $A(\tilde{\mathcal{R}}, \mathcal{S}_i)$, where $\tilde{\mathcal{R}}$ is the set of counterfactual RUC specialties given in Appendix Table A.7. Panel A plots the densities of counterfactual and actual distributions of affiliation. Panel B plots the densities of (i) the difference between counterfactual and actual affiliations for each proposal i , and (ii) the difference between actual and predicted affiliations for each proposal i , where predicted affiliation is a linear function of meeting dummies \mathbf{T}_t and specialty shares \mathbf{w}_i , as used in the baseline price regression in Equation (6). Panels C and D show the Q-Q plots that correspond to Panels A and B, respectively. These Q-Q plots display quantiles in the two distributions being compared; quantiles along 45-degree line indicate similarity between the two distributions.

Figure A.12: Principal Utility and Intermediary Bias



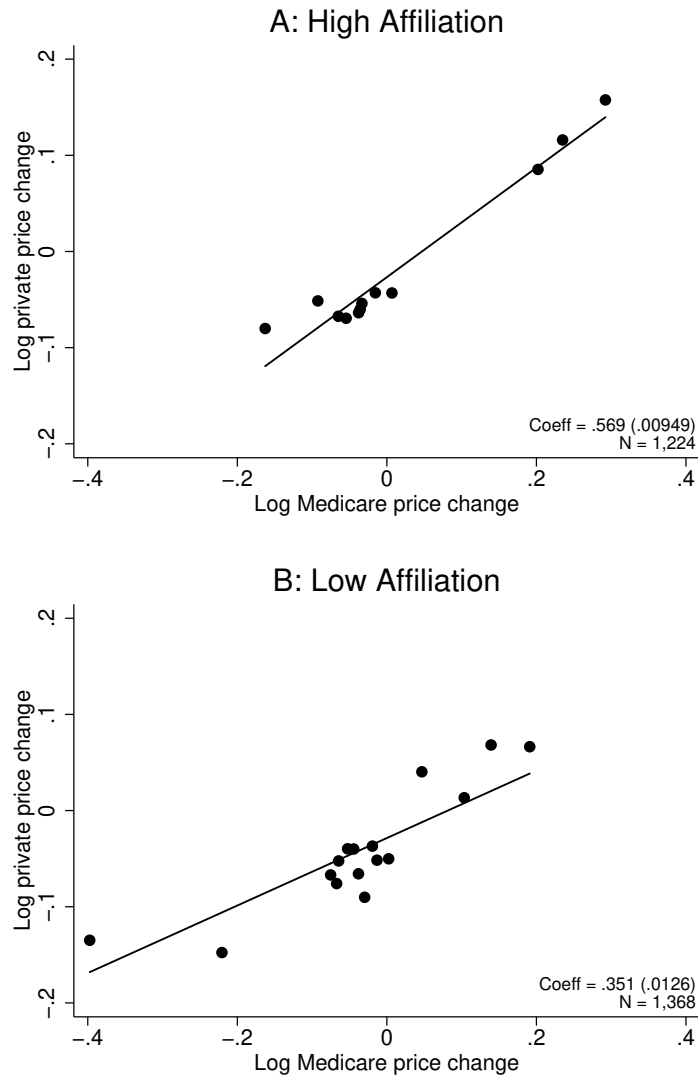
Notes: This figure shows the government utility (u_G) in our conceptual model of cheap talk, outlined in Section 5, in which the government delegates authority to the RUC as an intermediary to decide on proposals by a specialty society. The key parameter is bias of the RUC intermediary, b_R , where $b_R = 0$ indicates that the RUC has the same preferences as the government, and $b_R > 0$ indicates that the RUC is biased in favor of the specialty society, which prefers a higher price with bias $b_S > 0$. The figure shows $b_S = 0.3$ and $b_R \in [-0.1, 0.3]$, where $b_R = 0.3$ would imply RUC preferences identical to the specialty society. While greater b_R results in more distorted decisions (greater bias), greater b_R also improves communication. $b_R = 0$ only supports a babbling equilibrium with only one communication partition. The specialty society is able to invest in hard information, to reduce the size of the interval from $\theta \sim U(0, 1)$ to $\theta \sim U(\underline{\theta}, \bar{\theta})$, where $L \equiv \bar{\theta} - \theta$, at cost $c(L) = \kappa(1 - L)^2$. In both panels, u_G is shown in the case where $\kappa = \infty$ in dashed lines, and shows that the optimal b_R^* is between 0 and 1 (Dessein, 2002). Compared against this benchmark, Panel A shows costlier hard information ($\kappa = 1$), and Panel B shows cheaper hard information ($\kappa = 0.1$).

Figure A.13: Distribution of Normalized Log Medicare Price Changes



Notes: This figure shows the density of Medicare price changes associated with a RUC decision (solid line) or not (dashed line). Medicare prices are defined as the total payments divided by the total volume of claims for each CPT code and year pair observed in the 100% sample of Medicare claims. The figure excludes any pair with fewer than 10 claims. Log prices are then normalized by subtracting the average log Medicare price across CPT codes in a given year, weighted by frequency of claims. The figure plots the difference between the normalized log price for a CPT code in a year and the price for the same CPT code in the previous year.

Figure A.14: Private Price Changes on Medicare Price Changes



Notes: This figure is a binned scatterplot of log private price changes on log Medicare price changes arising from high-affiliation RUC proposals (Panel A) and low-affiliation RUC proposals (Panel B), where each dot represents 5% of the data, ordered by Medicare price change. Lines show the best fit through the data, and the line slopes correspond to coefficients on log Medicare price change in a univariate regression of log private price change. Coefficients are robust to regression controls similar to those in Table IV. For consistency with Table IV, observations are weighted by frequency of Medicare claims for a given service (CPT code). Unweighted observations yield higher coefficients of approximately 1.5 for high-affiliation RUC proposals and 1 for low-affiliation RUC proposals.